A STUDY OF GAS SOLUBILITIES AND TRANSPORT PROPERTIES IN FUEL CELL ELECTROLYTES

Research Grant NGL 10-005-022

Eleventh Semi-Annual Report

Period Covered: September 1, 1970 - February 28, 1971

CASE FILE COPY

ENGINEERING AND INDUSTRIAL EXPERIMENT STATION

College of Engineering

University of Florida

Gainesville

A STUDY OF GAS SOLUBILITIES AND TRANSPORT PROPERTIES IN FUEL CELL ELECTROLYTES

Research Grant NGL 10-005-022

Eleventh Semi-Annual Report

Period Covered: September 1, 1970 - February 28, 1971

Prepared for

National Aeronautics and Space Administration
Washington, D. C.

June 17, 1971

R. D. Walker, Jr.

ENGINEERING AND INDUSTRIAL EXPERIMENT STATION

College of Engineering
University of Florida
Gainesville, Florida

Table of Contents

Page

List of Tables

List of Figures

List of Symbols

c = Concentration in g mole/liter

d = Hard sphere diameter

f_i = Fugacity of component i

k = Boltzmann constant

M_i = Molality of component i

$\bar{M}$ = Concentration in total g ion/1000 gm solution

n_i = Number of g moles of component i

p_i = Partial pressure of component i

P = Vapor pressure

T = Absolute temperature

x = Mole fraction of electrolyte

$\phi(r)$ = Potential function

σ = Size parameter in potential function

$\nu_i = \frac{\text{Number of g ion of species i}}{\text{g mole of electrolyte}}$

1. Introduction

For the past six months, considerable efforts were made in the experimental measurements of:

(i) Vapor pressures of ternary electrolyte systems

(ii) Partial molal volumes of gases dissolved in electrolyte solutions

(iii) Diffusion coefficients of gases in electrolytes

Measurements of the vapor pressure using a differential manometer have proved to be very successful. The vapor pressure of the system KOH-K_2CO_3-H_2O was measured at 25, 40, 60 and 80°C over considerable concentration ranges of both KOH and K_2CO_3. It was found that the vapor pressure can be correlated for each temperature as a function dependent only on the ionic concentration.

Partial molal volume of gases in electrolyte solutions were measured for a wide variety of gases and ions. The dilatometric method of measuring partial molal volume was found to be an accurate, reliable and consistent method, provided care was taken in temperature and pressure controls. The results are comparable with literature values for gases in pure water; however, no comparison could be made for ionic solutions since for the systems studied no data exist. The results were discussed in light of the perturbation theory developed previously. Work on the measurement of the diffusion coefficients of hydrogen in lithium hydroxide solution was continued. Measurements were made for

the temperatures 25, 40, 60 and 80°C over the complete concentration range. The results are relatively well predicted by the modified Eyring theory and the kinetic theory.

2. Vapor Pressure in the System - Potassium Carbonate-Potassium Hydroxide-Water

A fuel cell is an electrochemical device composed of a non-consumable anode and cathode, an electrolyte, and suitable controls. The free energy of the reactants, which are stored outside the cell itself, is converted into electrical energy in the cell. Fundamentally, any oxidation-reduction reaction may be a potential fuel cell. Perhaps the most highly refined fuel cell system today is the human body, a mechanism that catalytically (enzymes) burns (oxidizes) food (fuel) in an electrolyte (cell fluid), to produce energy, some of which is electrical.

The hydrogen-oxygen fuel cell has been widely used; it employs a cathode at which hydrogen is oxidized, an anode at which oxygen is reduced, and an appropriate electrolyte. Since the oxygen electrode works best in an alkaline medium, potassium hydroxide is most often used as the electrolyte. Petroleum hydrocarbons would offer many advantages as a fuel but, since the oxidation products of hydrocarbons are carbon dioxide and water, the alkalinity of the electrolyte would be reduced through the formation of potassium carbonate. The result would be a ternary electrolyte system: $KOH-K_2CO_3-H_2O$.

It is also important to note that the vapor pressure of water will be an important property of any aqueous system. The vapor pressure is a temperature dependent quantity, and at the elevated temperatures normally employed for fuel cells to reduce electrode polarization the

vapor pressure will be substantial. Adequate vapor pressure data are not available for the potassium carbonate-potassium hydroxide-water system. Therefore a project to measure these vapor pressures was undertaken.

2.1 Thermodynamic Aspects

Consider a nonideal liquid solution in contact with a vapor phase. By the rule of phase equilibrium, the fugacities (or alternately, the chemical potentials) of each component are the same in all phases. Thus for any component i

$$f_i^G = f_i^L \tag{2-1}$$

where superscripts G and L refer to the gas and liquid phase, and f_i is the fugacity of component i. Near atmospheric pressure, the gas phase is essentially ideal and the vapor phase fugacity can be replaced by the partial pressure with minimal error

$$f_i^G = p_i \tag{2-2}$$

The fugacity in the liquid phase is given by

$$f_i^L = X_i \gamma_i f_i^S \tag{2-3}$$

where X_i is the mole fraction of component i, γ_i is the activity coefficient, and f_i^S is the standard state fugacity. For water the standard state is usually chosen to be pure liquid at the same temperature and pressure as the mixture; i.e., its pure component vapor pressure at the temperature of interest. Combining Equations 2-1, 2-2, and 2-3 with the above statement leads to

$$p_i = X_i \gamma_i P^o \tag{2-4}$$

where P^o is the pure component vapor pressure. In electrolyte systems of interest here, Equation 2-4 also describes the total vapor pressure, since the solutes are nonvolatile.

Thus, knowing vapor pressures, one can calculate activity coefficients which are important to many other measurements and calculations of thermodynamic properties. In terms of work here, it is necessary to know the vapor pressures of given solutions in order to measure or predict the solubility and diffusivity of oxygen or hydrogen in them.

2.2 Some Techniques for Measuring Vapor Pressures

Many techniques have been used at one time or another to measure vapor pressure. Three of these will be discussed here, namely, the isopiestic, the dew point, and the manometric methods.

2.2.1 Isopiestic Method

This technique, first described by Bousfeld[1] in 1918 and later improved by Sinclair,[2] is a comparative method depending on the principle that two solutions of nonvolatile solutes will distill from one another until their concentrations are such that the solutions have equal vapor pressure. One of the solutions must have a well-known concentration and temperature vapor pressure dependency.

This can be done one of two ways, with perfect insulation between the solutions or with perfect thermal contact. Let A and B be two solutions, the vapor pressure of A being initially greater than that of B. Then solvent will distill from A to B, thus cooling A by its vaporization and heating B by its condensation. Because of the temperature changes, the vapor pressure of B increases, while the vapor pressure of A decreases. Were perfect thermal insulation maintained between the solutions, a steady state would result with a temperature difference between the solutions sufficient to equalize the vapor pressures. Recording temperatures of both solutions and analyzing for their concentration allows one to ascertain the vapor pressure of the unknown solution at the given temperature and concentration.

At the other extreme the above procedure can be carried out with perfect thermal contact. In this case, the vapor pressure of A decreases, and the vapor pressure of B increases, not as a result of a temperature difference, but because of a concentration difference. Equilibrium results when this concentration difference suffices to equalize the vapor pressure. After analysis of both solutions, one again can ascertain the vapor pressure of the unknown solution at the given temperature (the same for both solutions) and concentration.

2.2.2 Dew Point Method

This method, first described by Cumming[3] and modified by Walker,[4] depends on measuring the dew point of a sample very accurately. In practice a container contains solution, above which is suspended a highly polished silver tube. The apparatus is lowered into a constant temperature bath and a vacuum is drawn on the system. This method does not require a vacuum, but the appearance of dew on the silver tube is enhanced when air does not interfere. The silver tube has provisions for water from another bath to be circulated through it. The temperature of the silver tube is slowly reduced until dew forms on it, the temperature of first dew formation being recorded. Then the temperature is increased until the dew disappears. These two temperatures should be identical; in practice, they usually differ slightly and an average is taken for calculation of the vapor pressures. The vapor pressure of the sample solution at the temperature of the bath (the one containing the apparatus) is thus the vapor pressure of water at the dew point of that solution (the temperature of the silver tube at the initial formation of dew).

2.2.3 Manometric Method

This method employs a direct measurement of the pressure exerted by the solution. It will be described here briefly; a more detailed discussion will be found in Section 2.3. In general, this method may be used in the absolute or the differential mode. In the first, the vapor pressure of the solution is measured against a vacuum, in the second, against a known standard solution. The two solutions, in a constant temperature bath, are connected to the two arms of a manometer. The system is evacuated (in this method a vacuum is necessary, since nothing but water vapor should exist in the vapor space). Once the system is evacuated, the solutions are allowed to equilibrate with their respective vapor spaces. Thus, the pressure in the vapor space is the vapor pressure of the solution. The difference in the level of the fluid in the arms of the manometer is a measure of the difference in the vapor pressures in the two vessels.

2.3 Apparatus and Experimental Procedure

The apparatus is pictured in Figure 2.1. It consists of a Gilmont micrometric manometer suitably modified to be connected to sample containers and a vacuum pump. The constant temperature environment, in which the manometric assembly is housed, consists of an insulated water bath containing heaters, a stirrer, and a temperature probe, all connected to a proportional controller. The two thermometers used were readable to 0.01°C and were calibrated against a quartz thermometer. Bath temperatures could be controlled to ±0.01°C at 25°C and better than ±0.1°C at 80°C. Mercury used was triple distilled and was changed every few runs due to water deposition on its surface.

The Gilmont micrometric manometer employs a stainless steel needle connected to a micrometer to measure the height of the mercury column. The micrometer is readable to 0.0005" which is approximately 0.01 mm. The standard tapered male joints and the tubing culminating in the three-way stopcock were added by the glassblower, while the special mounting apparatus of Plexiglass and metal was fashioned in the machine shop.

Twenty-five different solutions of potassium carbonate, potassium hydroxide and water were prepared. These were calculated to evenly cover the entire solubility range of the system at 25°C. The KOH used was Fisher reagent grade pellets, low in chloride, but containing about

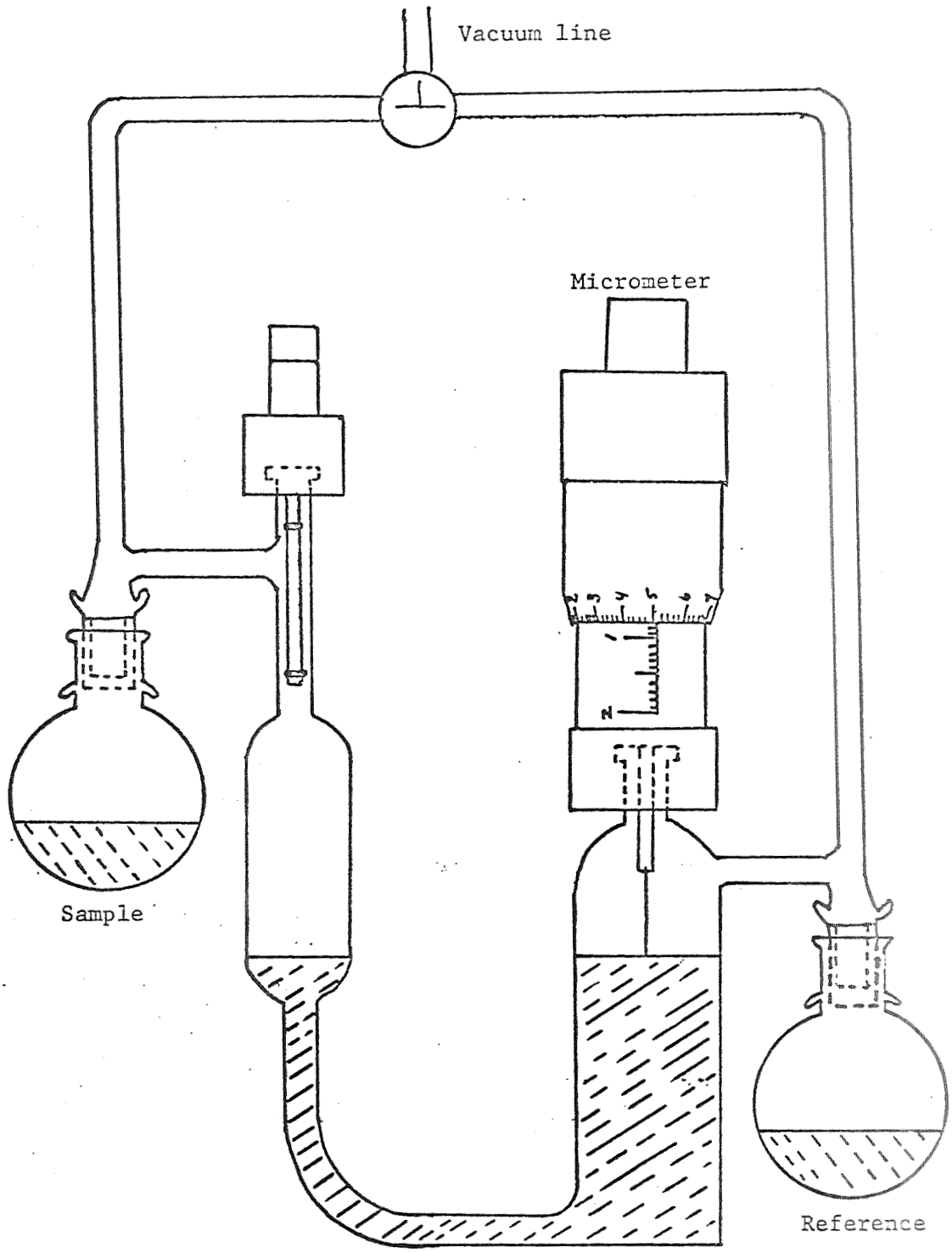

Figure 2.1. Manometric Assembly

one percent K_2CO_3. The K_2CO_3 was Fisher reagent grade granular anhydrous. The water used was deionized and then distilled.

Amounts of KOH and K_2CO_3 that were calculated to give the proper concentration were weighed out to the nearest 0.1 gram and transferred into a liter volumetric flask. Water was added and the solids were allowed to dissolve. The flask was then cooled to room temperature and filled to the mark with water. Solutions were kept no longer than necessary in glass containers since KOH has a deleterious effect on glass; they were stored in brown opaque Nalgene bottles with screw tops.

Once mixed, the solutions were analyzed. Two analyses are required on a sample to determine the carbonate and hydroxide content: one for total alkalinity and one for hydroxide.

The sample was placed in a dropping bottle and the dropping bottle plus sample was weighed on an analytical balance to the nearest 0.1 mg. Then approximately 1 to 5 grams (depending on the sample concentration) of sample was transferred to a 400 ml beaker containing deionized, distilled water. The sample was then reweighed and the difference in weight recorded as the sample size.

The standard acid, 1.0 N HCl, was prepared by diluting special ampules of Acculute concentrated acid to one liter. It was kept in a four-liter flask which was connected to a self-filling, self-zeroing burette with provisions for slow and fast delivery. The acid was protected from atmospheric contamination by a glass tube containing activated silica gel dessicant to exclude both water vapor or carbon dioxide.

To measure total alkalinity the sample was titrated with standard HCl with a bromcresol green indicator. Bromcresol green is blue in basic media, green in transition, and yellow in acidic media. The sample was titrated until just before the end point. It was then boiled to drive out the CO_2 (formed from the carbonic acid formed in the HCl, K_2CO_3 reaction); this sharpens the end point. After cooling, the titration is completed. The total equivalents of carbonate plus hydroxide is determined in this analysis.

To measure total hydroxide content, the carbonate is first precipitated by adding barium chloride solution. Since barium hydroxide is soluble while barium carbonate is not, the hydroxide remains in solution. The sample thus prepared is titrated with standard HCl with a phenolphthalein indicator. The endpoint is reached when the solution changes from pink to white (not clear because the precipitate remains suspended). This gives total equivalents of hydroxide. From these two analyses, one determines amount of K_2CO_3 and KOH in the sample. All analyses were done in triplicate, thus six analyses were necessary for each sample. A sample calculation is presented in the Appendix. The solution compositions are presented in Table 2.1 and Figure 2.2.

In the vapor pressure measurements, the bath was first brought to the desired temperature. The manometer was filled with mercury and zeroed. A special high temperature stopcock lubricant was applied to all joints in the system, including the three-way stopcock, the vacuum hose connector, and the standard tapered joints which connected the sample flasks with the main assembly. The lubricant was wiped off and renewed every run on

Table 2.1: Solution Names and Compositions

Name	Wt. Pct. KOH	Wt. Pct. K_2CO_3
1A	4.18	4.84
1C	11.78	4.62
1E	18.68	4.36
1G	24.40	4.43
1J	30.19	4.39
1N	40.55	4.30
1P	45.01	4.05
3A	4.14	10.91
3C	11.00	12.96
3E	17.85	11.46
3G	23.28	12.57
3L	33.52	11.46
5A	3.57	21.90
5C	10.50	20.95
5E	16.38	20.46
5G	23.21	19.37
7A	3.25	28.25
7C	9.94	27.88
7E	15.60	27.10
7G	21.09	25.99
9A	3.17	33.59
9C	9.44	34.04
9E	15.30	32.89
11A	3.31	41.31
11C	9.11	39.91

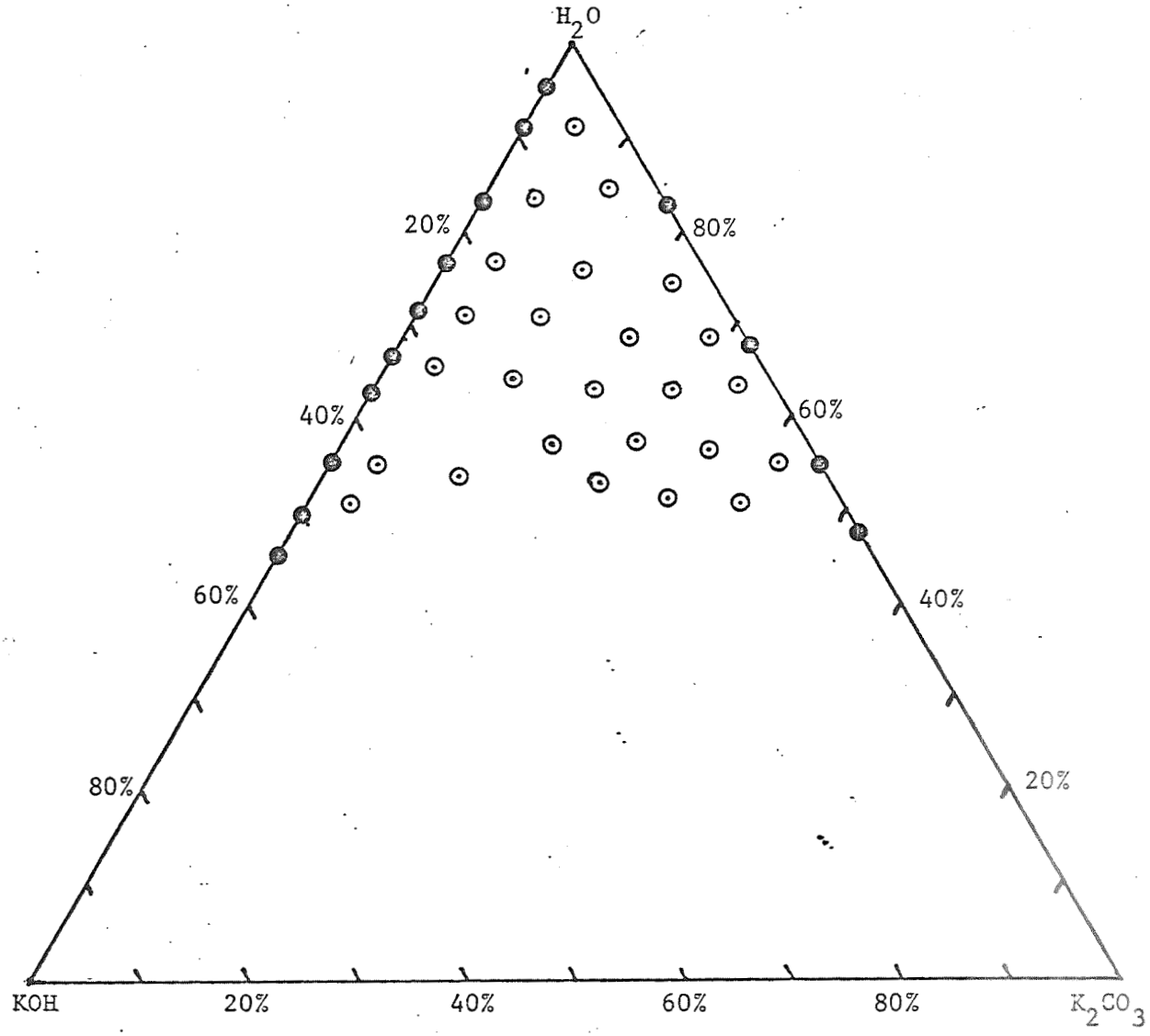

Figure 2.2. Solution Compositions

the standard tapered joints and as often as necessary on the other moving parts.

The right hand sample flask was filled with deionized, distilled water and attached to the main assembly with rubber bands. Sample was poured into the left hand sample flask. After this the manometric assembly was lowered into the bath and the vacuum hose was attached.

The system was evacuated, first on the right hand flask then on the left hand flask. They were then allowed to equilibrate with each other. This was repeated several times. The purpose of this was first to purge the dissolved gases from the solutions and later to remove all traces of air from the vapor space. When this was accomplished, the three-way stopcock was turned skew so as to separate the vacuum line from the manometer and the two arms from each other.

Readings were taken every five minutes until equilibrium was reached. This required anywhere between fifteen minutes and ninety minutes depending on the temperature and the sample. There are two equilibria which must be reached here; (1) the vapor and liquid must equilibrate with each other and (2) the system must equilibrate (temperature-wise) with the bath. Because of the limited scale of the manometer (2") many of the samples at higher temperatures were run against previously established standards rather than water. This added somewhat to the experimental error.

It was necessary to first boil a solution to purge the air from the vapor space. The solution composition was changed slightly by vaporizing some of the original liquid water. Thus a few samples were

analyzed before and after an experimental run. The differences in composition were found to be negligible and this practice was discontinued for future runs.

2.4 Methods of Data Treatment and Correlation

2.4.1 Methods Used by Other Investigators

Two methods have been previously investigated as to the prediction and/or correlation of strong ternary electrolyte vapor pressures. One method, which interpolates, is usable only for predicting a value of vapor pressure when many points are known. And since strong ternary electrolyte vapor pressure is a function of three variables (two concentrations and temperature), the interpolation can become quite complicated and inaccurate. As an added disadvantage, adequate vapor pressure data are available for only a few systems.

This has led certain investigators[5] to postulate that ternary vapor pressures could be predicted from binary system data. The following equation has been suggested

$$P = \frac{M_1 P_1 + M_2 P_2}{M_1 + M_2} \qquad (2\text{-}5)$$

where: P = vapor pressure of the ternary

M_1 = molality of component 1

M_2 = molality of component 2

P_1 = vapor pressure of binary 1

P_2 = vapor pressure of binary 2

This method has been discussed in previous NASA reports.[6] Its major drawback is that the component molalities are calculated before mixing.

Thus some ternary solutions may exist for which binary data would have to be extrapolated; the method does actually break down in this case. Its general accuracy is also not particularly good. Actual experimental values vs. values predicted by this method are presented in Table 2.2.

2.4.2 Methods Used in This Report

2.4.2.1 Screening of Experimental Data for Consistency

The experimental data are presented in Table 2.3. The experimental data were first examined for internal consistency. Each data point was plotted on a ℓn P vs. 1/T graph as shown in Figures 2.3 through 2.8. If a point deviated significantly from the straight line, it was discarded and the experiment rerun. The points were then fitted to an equation of the form $\ell n\ P = A + B/T + C/T^2$. The coefficients along with those derived from curves fitted to vapor pressures of binary solutions are presented in Table 2.4.

2.4.2.2 Deriving a Best Fit

The same problem was encountered with this method as was encountered with the Antoine equation ($\ell n\ P = A + B/T + C$); i.e., while each solution was fitted very well by the individual coefficients, no temperature dependence of the coefficients could be ascertained. They exhibited a general upward trend with increasing concentration but deviated substantially from any functional form. It was possible to fit them, but the resultant equation was so inaccurate as to be useless. This approach was, therefore, abandoned.

As has been pointed out before, vapor pressure in strong ternary electrolyte systems is a function of three variables. It seemed that the most promising approach would be to find a combining rule which

Table 2.2: Additivity of Molalities Correlation vs. Experimental Points

	25°		40°		60°		80°	
SOLUTION	EXP	CORR	EXP	CORR	EXP	CORR	EXP	CORR
1A	22.6	22.4	52.1	51.8	141.5	140.2	341.0	334.1
1C	20.8	18.7	48.4	43.6	129.6	116.5	316.5	279.4
1E	17.1	13.5	40.4	31.1	119.6	86.1	283.1	208.0
1G	15.1	9.19	35.5	21.5	101.5	60.1	245.2	147.3
1J	11.9	5.60	28.3	10.5	84.0	38.1	203.4	97.4
IN	5.15	1.80*	14.7	4.41*	49.7	12.8*	135.5	34.1*
1P	4.18	1.12*	11.0	2.59*	38.8	7.40*	108.1	19.8*
3A	22.1	21.8	50.7	50.5	138.5	138	330.2	328.0
3C	20.0	18.9	45.6	44.1	121.1	118.2	295.6	283.2
3E	16.0	14.0	38.7	32.5	106.6	89.0	260.6	214.7
3G	12.5	9.75*	30.9	22.9*	84.5	63.8*	215.0	155.3*
3L	7.07	4.28*	16.5	10.1*	52.5	29.0*	142.6	74.0*
5A	20.9	19.1	47.5	44.5	129.0	120.2	307.0	289.8
5C	17.6	18.0	41.0	42.0	110.2	112.4	269.6	271.2
5E	13.6	13.8	32.6	32.1	89.5	88.4	226.7	213.6
5G	10.6	8.83*	25.5	21.0*	71.8	59.0*	180.6	147.0*
7A	18.1	16.2	43.3	38.0	118.0	104.1	288.6	292.4
7C	15.8	15.8	35.6	36.8	98.4	99.4	241.7	270.0
7E	11.7	12.0	28.5	27.6	79.8	76.1	198.7	210.6
7G	8.6	8.33*	21.1	19.9*	61.8	55.3*	157.1	159.0*
9A	16.8	13.4	38.2	31.6	103.7	86.9	253.2	217.9
9C	13.0	12.3*	31.3	29.0*	84.0	80.2*	208.1	200.5*
9E	9.8	9.55*	23.1	22.4*	64.3	63.0*	162.2	159.6*
11A	13.1	9.02*	32.7	21.3*	97.1	59.3*	253.0	155.6*
11C	10.9	9.41*	26.2	22.4*	77.6	62.3*	197.0	158.4*

*Extrapolated

Table 2.3: Experimental Vapor Pressures of Solutions

Solution	Vapor Pressures At: 25°	40°	60°	80°
H_2O	23.76	55.32	149.19	355.1
1A	22.6	52.1	141.5	341.0
1C	20.8	48.4	129.6	316.5
1E	17.1	40.4	119.6	283.1
1G	15.1	35.5	101.5	245.2
1J	11.9	28.3	84.0	203.4
IN	5.15	14.7	49.7	135.5
1P	4.18	11.0	38.8	108.1
3A	22.1	50.7	138.5	330.2
3C	20.0	45.6	121.1	295.6
3E	16.0	38.7	106.6	260.6
3G	12.5	30.9	84.5	215.0
3L	7.07	16.5	52.5	142.6
5A	20.9	47.5	129.0	307.0
5C	17.6	41.0	110.2	269.6
5E	13.6	32.6	89.5	226.7
5G	10.6	25.5	71.8	180.6
7A	18.1	43.3	118.0	288.6
7C	15.8	35.6	98.4	241.7
7E	11.7	28.5	79.8	198.7
7G	8.6	21.1	61.8	157.1
9A	16.8	38.2	103.7	253.2
9C	13.0	31.3	84.0	208.1
9E	9.8	23.1	64.3	162.2
11A	13.1	32.7	97.1	253.0
11C	10.9	26.2	77.6	197.0

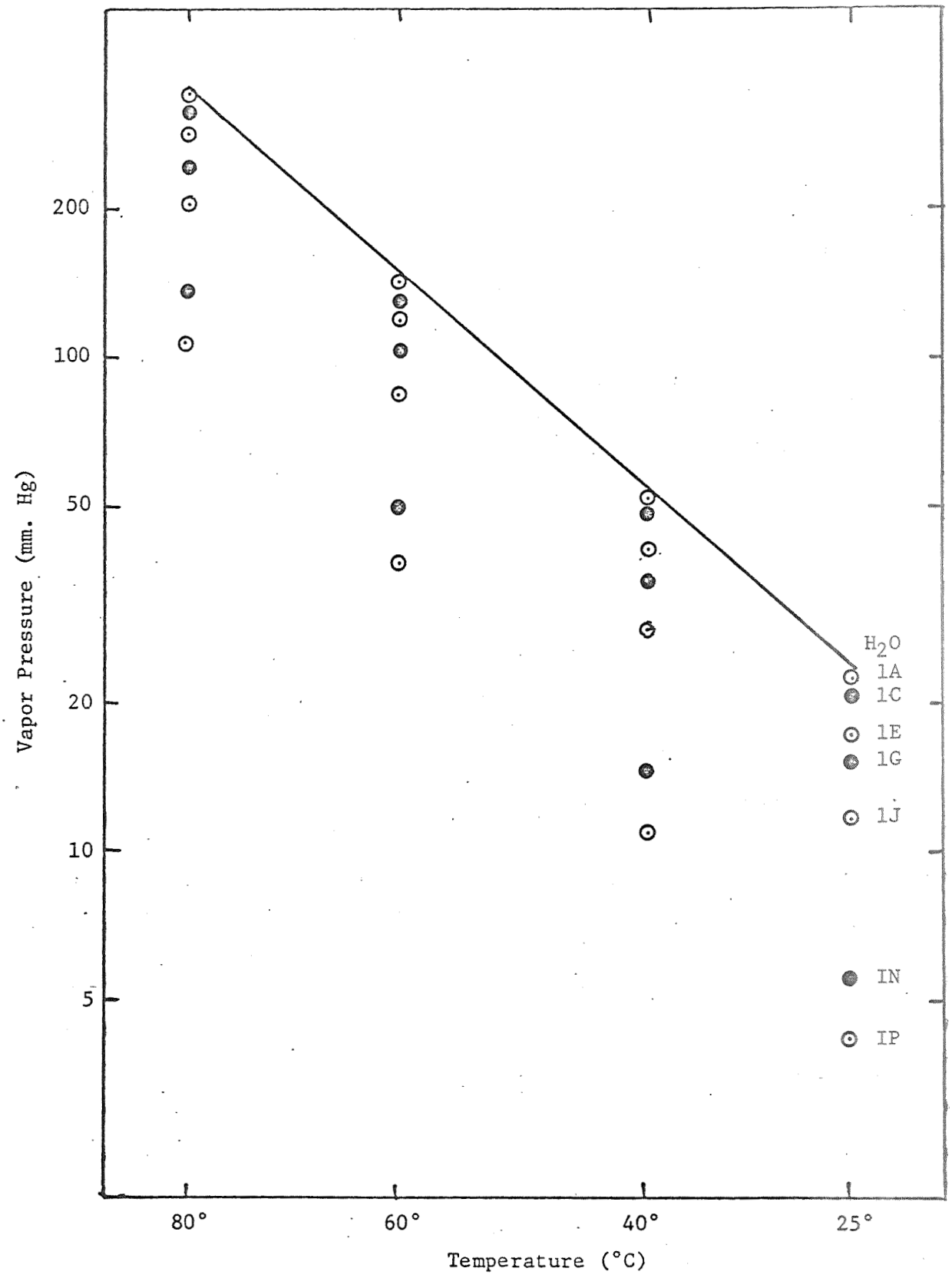

Figure 2.3. Experimental Vapor Pressures

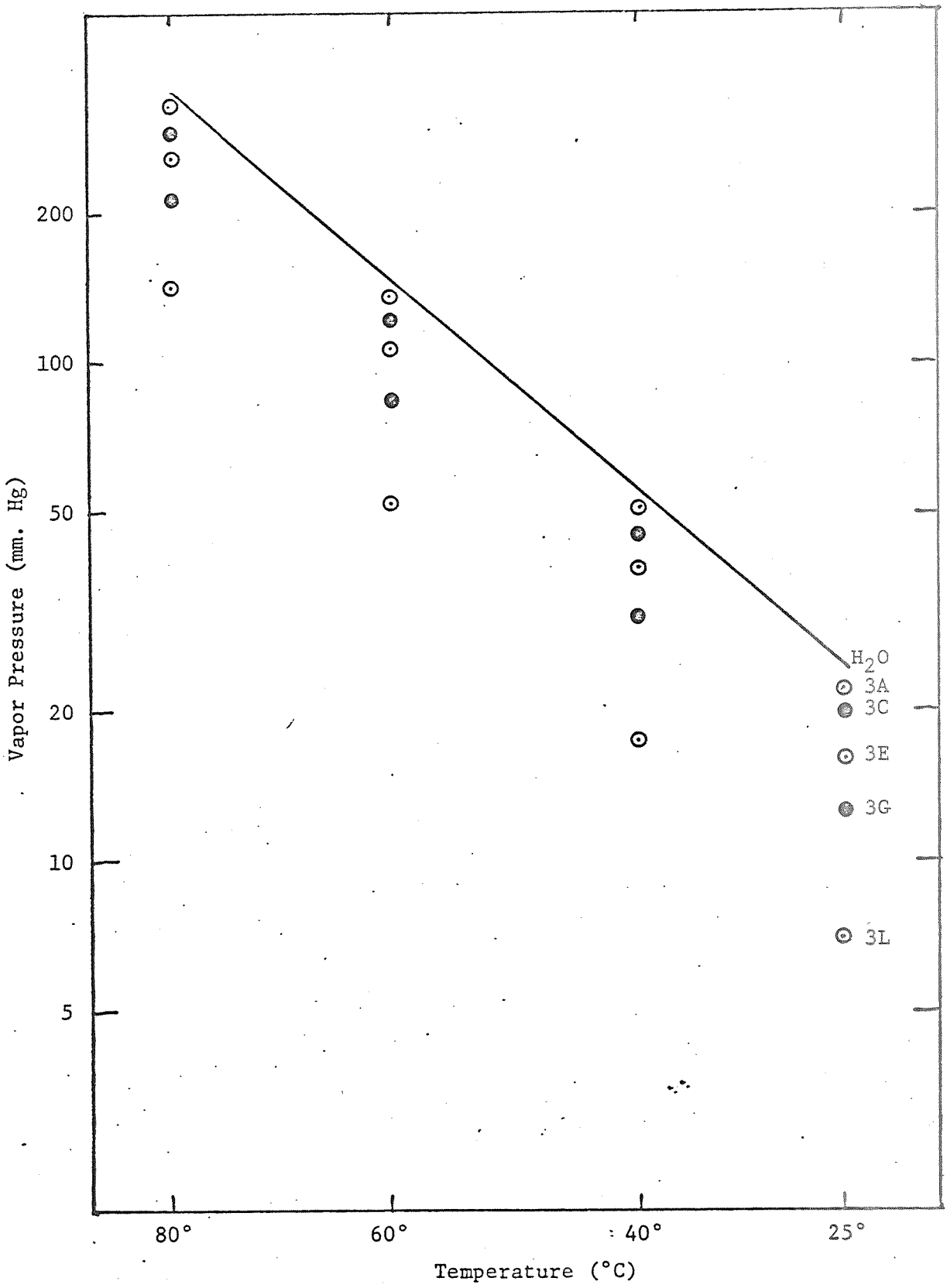

Figure 2.4 . Experimental Vapor Pressures

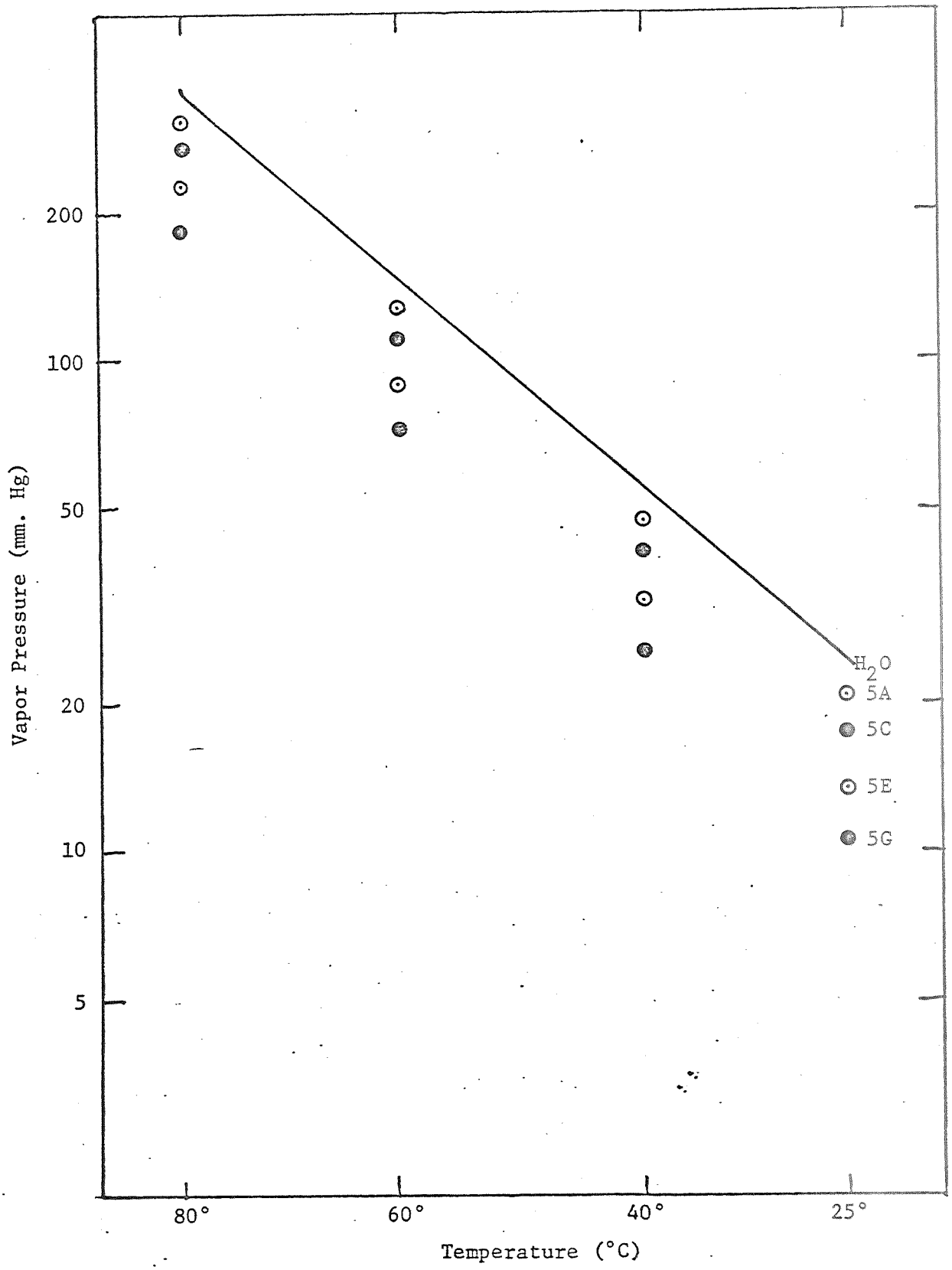

Figure 2:5. Experimental Vapor Pressures

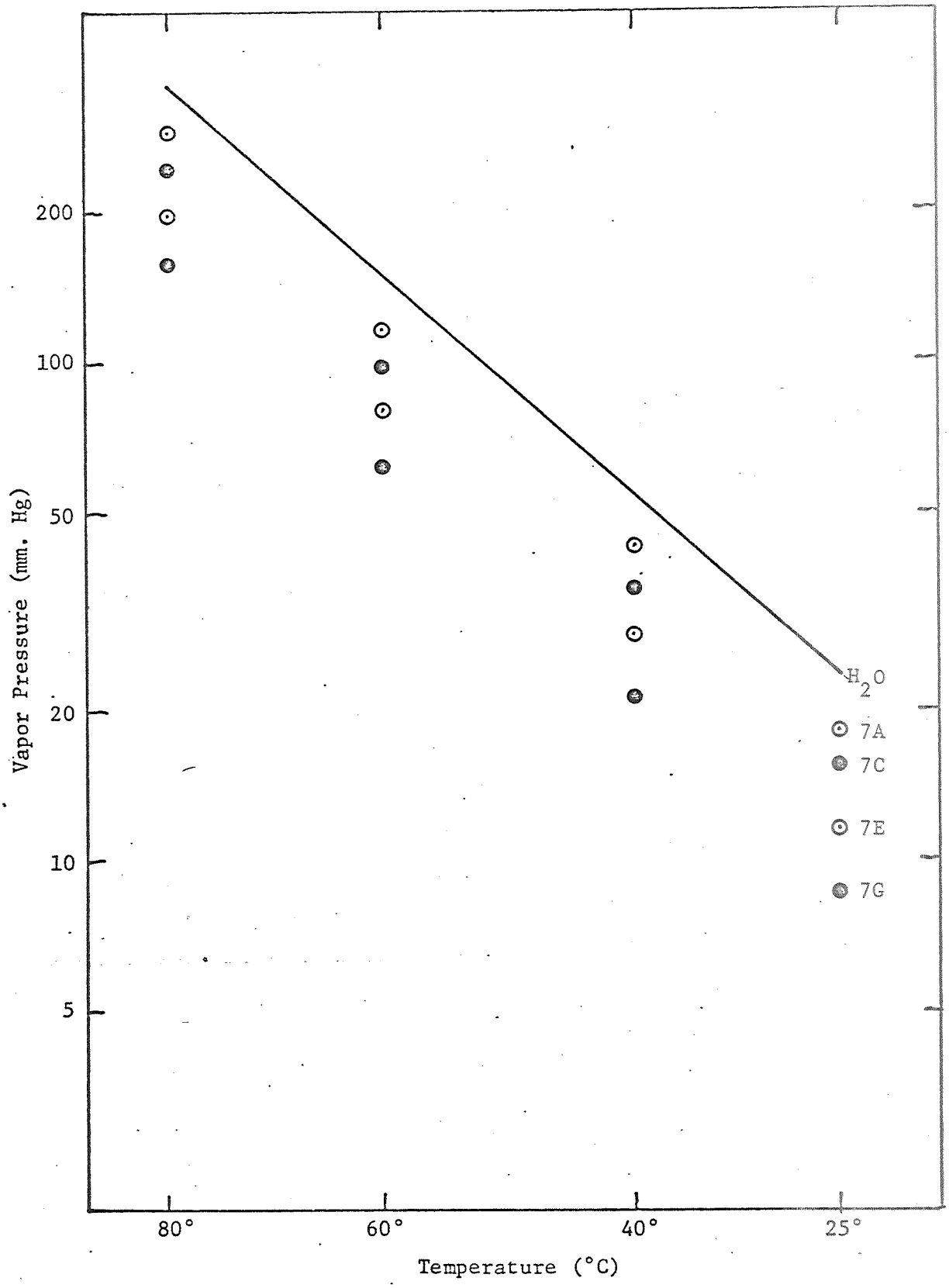

Figure 2.6. Experimental Vapor Pressures

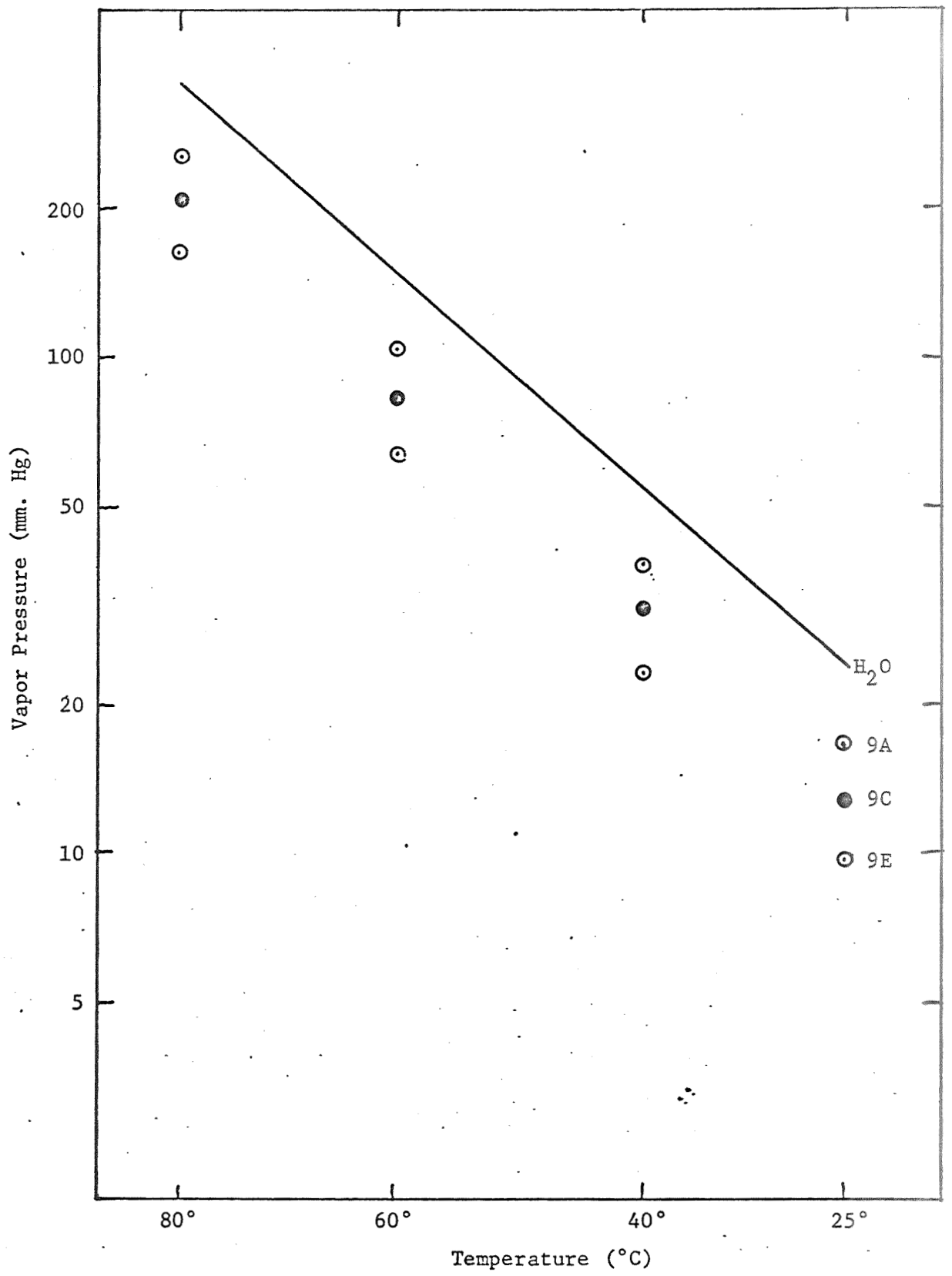

Figure 2.7. Experimental Vapor Pressures

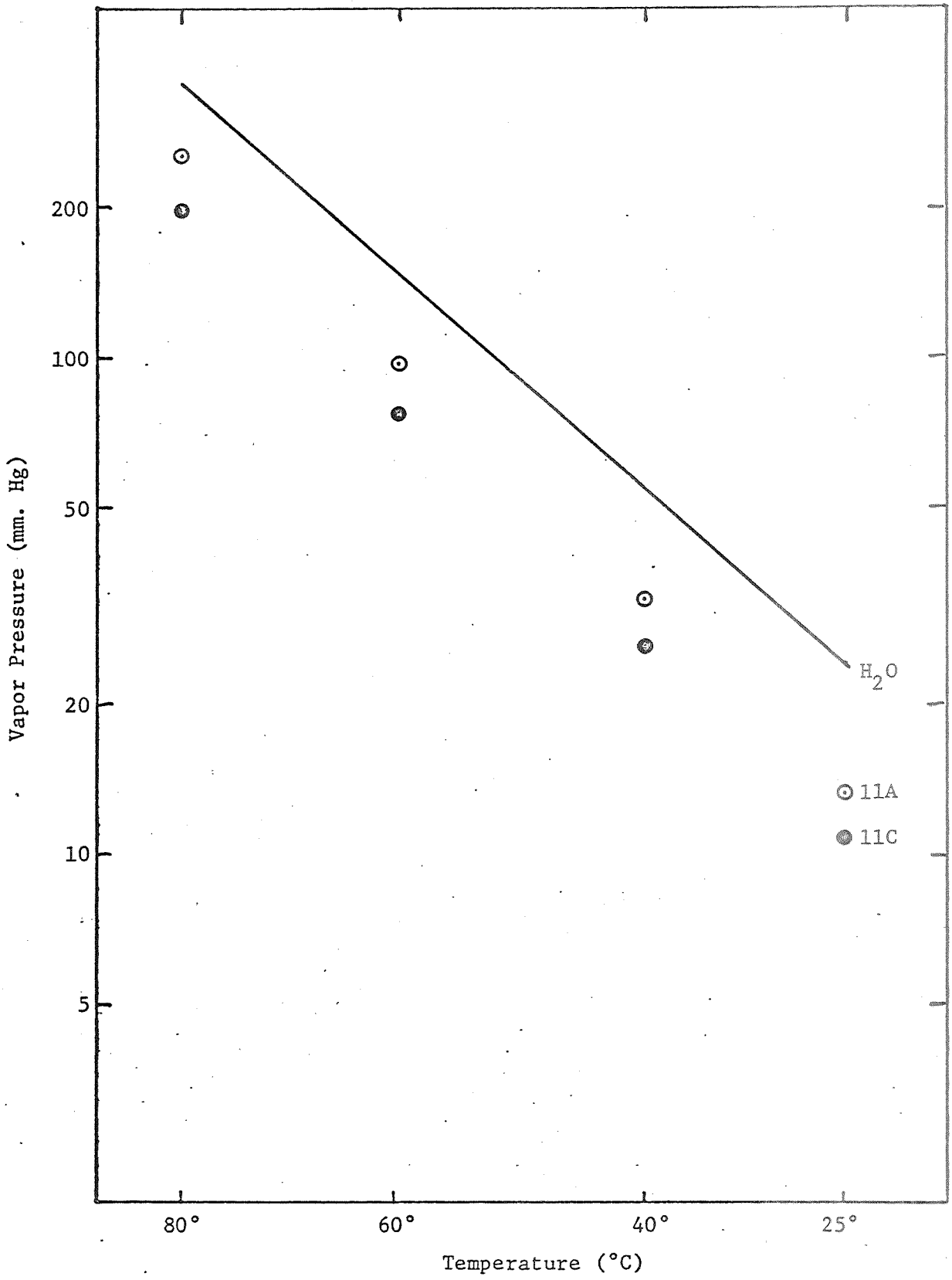

Figure 2.8. Experimental Vapor Pressures

Table 2.4: Coefficients Used to Fit Solutions to Equation $\ln P = A + \frac{B}{T} + \frac{C}{T^2}$

Solution	A	B	C
1A	20.285	-5024.9	-27955
1C	20.577	-5260.8	9285.7
1E	16.970	-2804.7	-420760
1G	18.851	-4171.9	-191020
1J	18.169	-3755.0	-276130
1N	14.384	- 875.16	-872290
1P	22.353	-6209.2	-9652.1
3A	19.840	-4765.6	-67777
3C	22.052	-6311.2	187830
3E	17.672	-3383.2	-315580
3G	19.172	-4414.2	-163080
3L	29.331	-10982	839860
5A	20.264	-5116.4	-5848.6
5C	20.533	-5324.9	17452
5E	21.255	-5777.5	65443
5G	20.240	-52183	-33451
7A	18.605	-3960.6	-215380
7C	23.419	-7259.6	327740
7E	18.469	-4010.8	-227190
7G	19.549	-4737.9	-134040
9A	22.295	-6529.2	215550
9C	18.856	-4341.1	-153420
9E	21.818	-6363.2	160660
11A	20.906	-5225.7	-71749
11C	21.238	-5757.0	32476

would output a new concentration variable that took into account both previous concentrations. This would reduce the equation to two variables and thus simplify the analysis.

Several combining rules were tried but all seemed to exhibit a systematic scatter. That is, when the vapor pressure was plotted versus new concentration variable, solutions containing large amounts of one component deviated systematically to one side of the line, while solutions containing large amounts of the other component deviated to the other side. A breakthrough was achieved when the concentration variable of total gram ions/1000 grams solution was tried. Calculation of this variable is presented in the Appendix.

When concentrations calculated in this manner were plotted versus vapor pressure, all the points fit a smooth curve, and scatter was random (due presumably to experimental error) rather than the systematic scatter described before. Binary systems also fit these curves, thus lending additional credence to this approach. These are shown in Figures 2-9 through 2-12.

Since the method seemed to correlate the data well, the next step was to fit a curve to the data points. The value of the new concentration variable is presented in Table 2-5. A computer program was written to fit a polynomial of any desired degree to the data. This curve is also shown in the above mentioned figures. The program is presented in the Appendix. By suitable manipulation of the variables it was also possible to fit logarithmic and reciprocal terms. Best results were obtained with a cubic equation in concentration versus the logarithm of vapor pressure

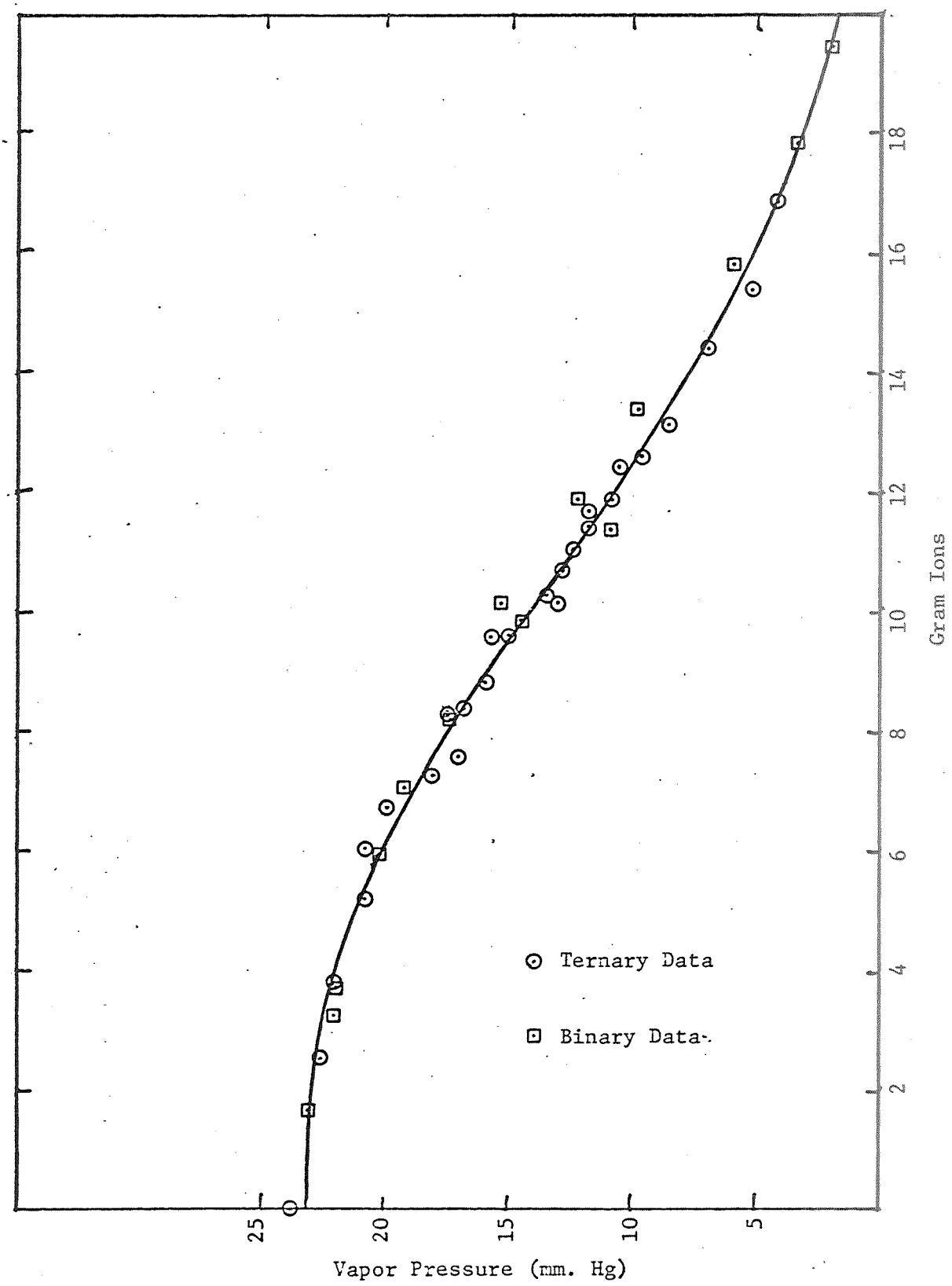

Figure 2.9. Concentration Dependence of Vapor Pressure at 25°C

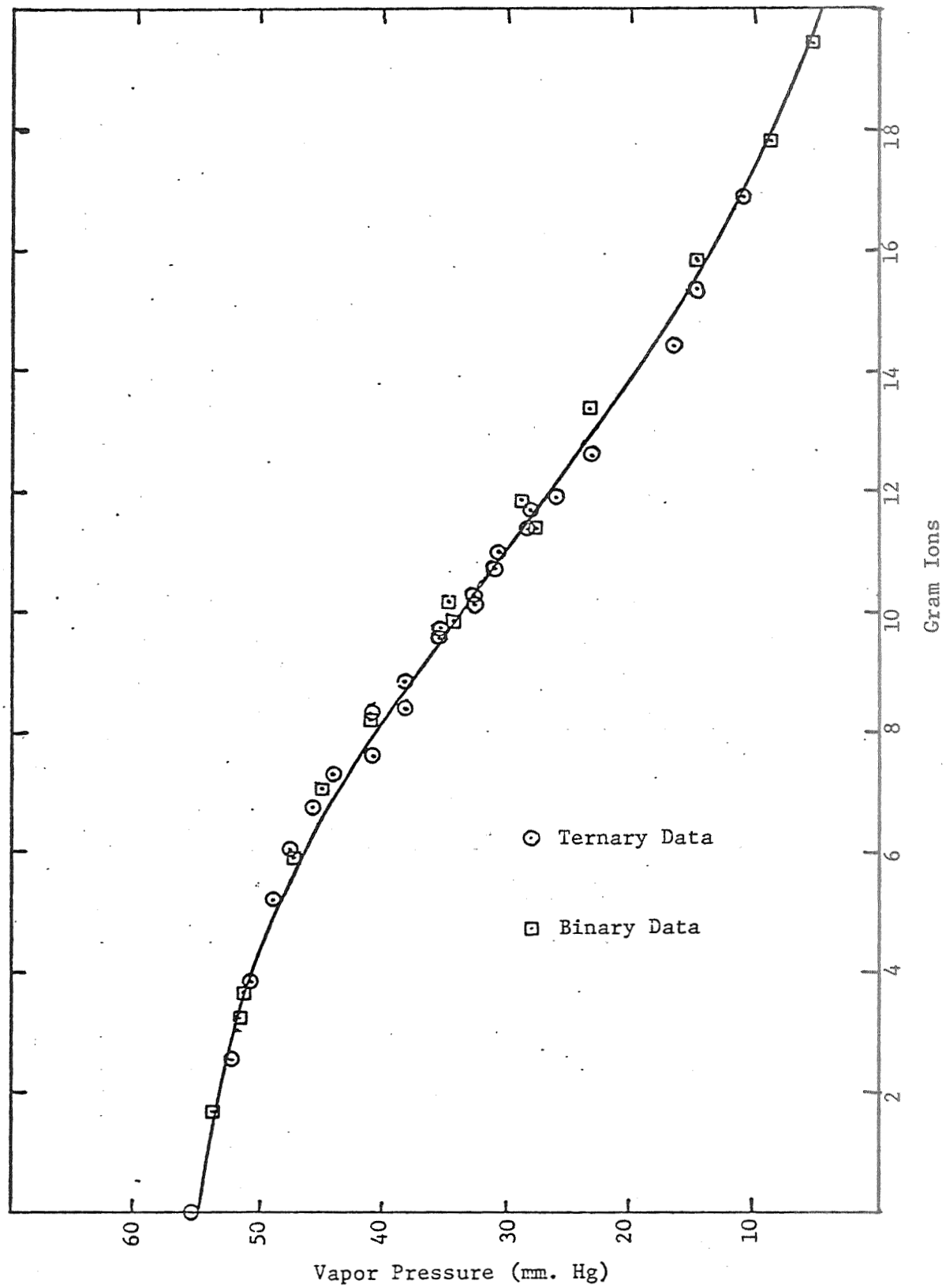

Figure 2.10. Concentration Dependence of Vapor Pressure at 40°C

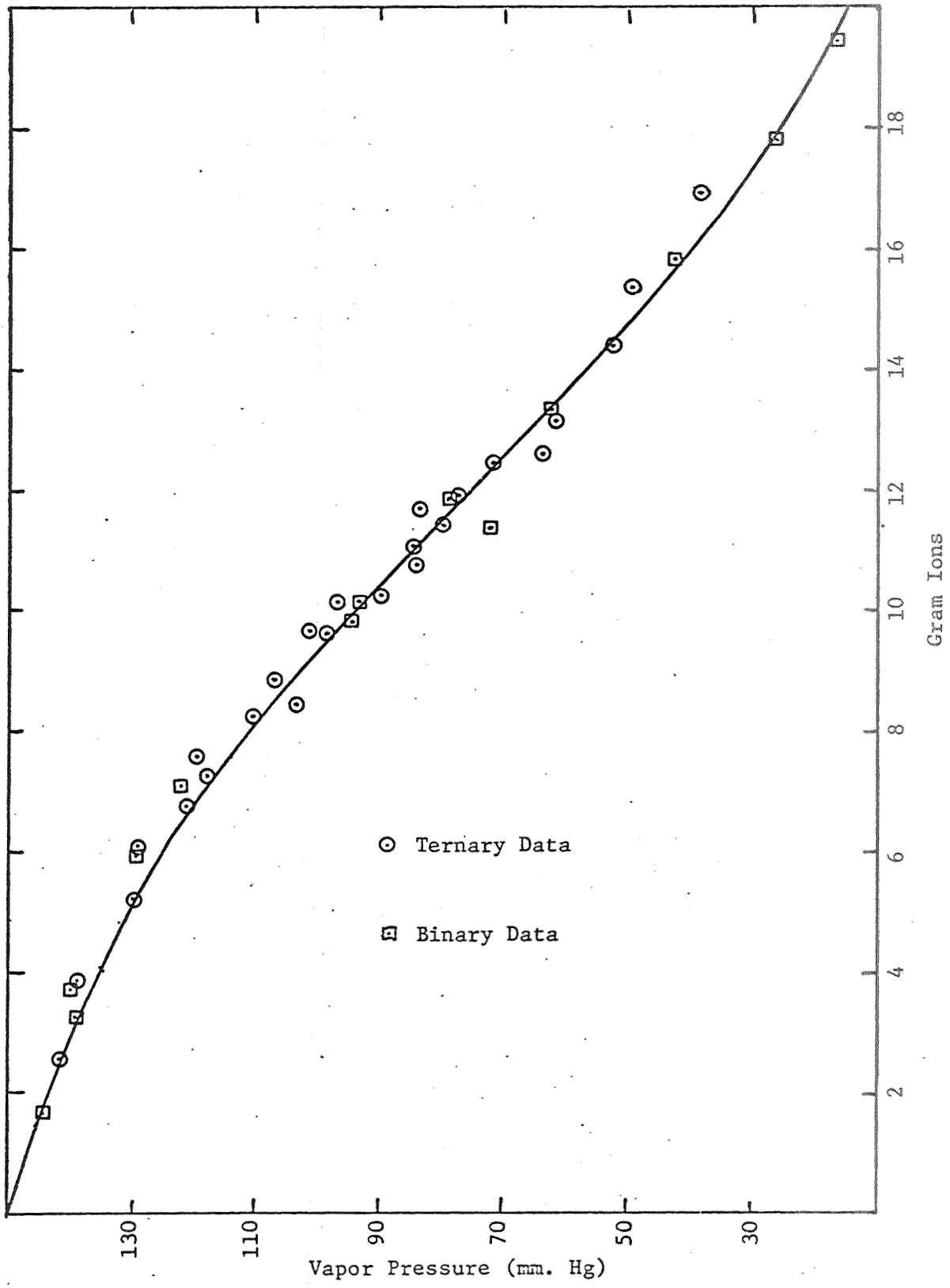

Figure 2.11. Concentration Dependence of Vapor Pressure at 60°C

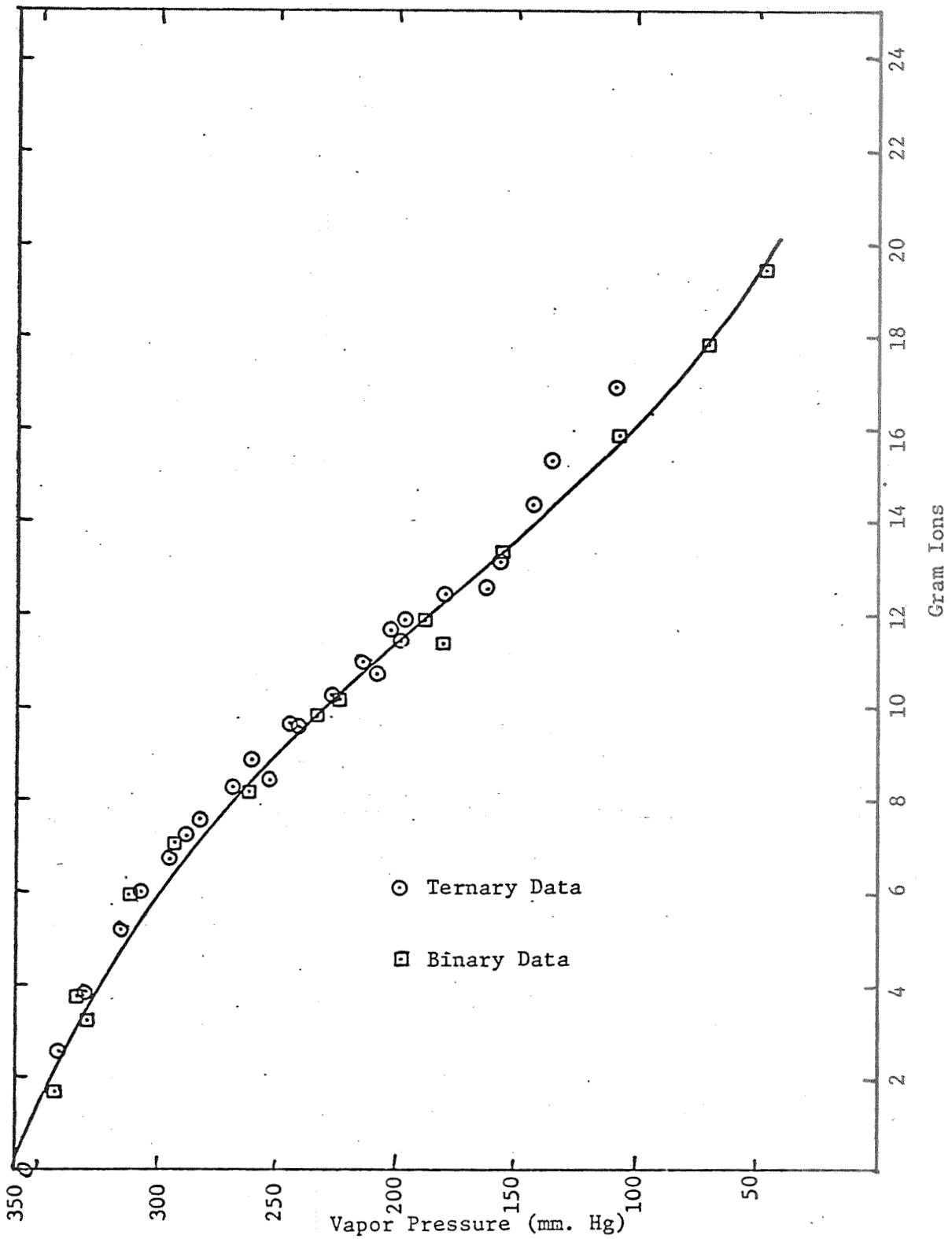

Figure 2.12 . Concentration Dependence of Vapor Pressure at 80°C

Table 2.5: Value of Total Gram Ions/1000 Grams Solution

SOLUTION	TGI	SOLUTION	TGI
1A	2.54	5C	8.29
1C	5.20	5E	10.28
1E	7.60	5G	12.48
1G	9.66	7A	7.29
1J	11.71	7C	9.60
IN	15.39	7E	11.44
1P	16.92	7G	13.16
3A	3.84	9A	8.42
3C	6.73	9C	10.75
3E	8.85	9E	12.59
3G	11.03	11A	10.15
3L	14.44	11C	11.91
5A	6.03		

$$\ell n\ P = A + B\bar{M} + C\bar{M}^2 + D\bar{M}^3$$

where A, B, C, and D are the coefficients. They were constant for a given temperature and all concentrations.

The coefficients have a definite value for each temperature for which data was taken. This is shown in Table 2.6. The next step was to determine the temperature dependence of the coefficients. It was found that it could be represented by a simple function of temperature.

Polynomial least squares fits were performed on the original A, B, C, D coefficients and functional forms were derived for their temperature dependence. The same subroutine was used as previously to fit the data. Curves of A, B, C, D versus temperature are presented in Figures 2.13 through 2.16 . The best fit line through the coefficients is also plotted in the above figures.

From these procedures a final equation was developed

$$\ell n\ P = A + B\bar{M} + C\bar{M}^2 + D\bar{M}^3$$

where A, B, C, D are now temperature dependent and have the following form:

$$A = A_1 + A_2/T + A_3/T^2$$
$$B = B_1 + B_2T + B_3T^2$$
$$C = C_1 + C_2T + C_3T^2$$
$$D = D_1 + D_2T + D_3T^2$$

These values are presented in Table 2.7.

As an added check, vapor pressures were calculated for each solution at temperatures of 30°, 50°, and 70° by means of the original

Table 2.6: Values of Coefficients of Equation $\ell n\ P = A + B\bar{M} + C\bar{M}^2 + D\bar{M}^3$

Temp	A	B	C	D
25°	3.1419	9.3469×10^{-3}	-46.764×10^{-4}	-1.0452×10^{-4}
40°	3.9994	-2.1853×10^{-3}	-30.902×10^{-4}	-1.4434×10^{-4}
60°	5.0153	-17.7410×10^{-3}	-8.9406×10^{-4}	-1.9669×10^{-4}
80°	5.8906	-22.8035×10^{-3}	$-.5988 \times 10^{-4}$	-2.1366×10^{-4}

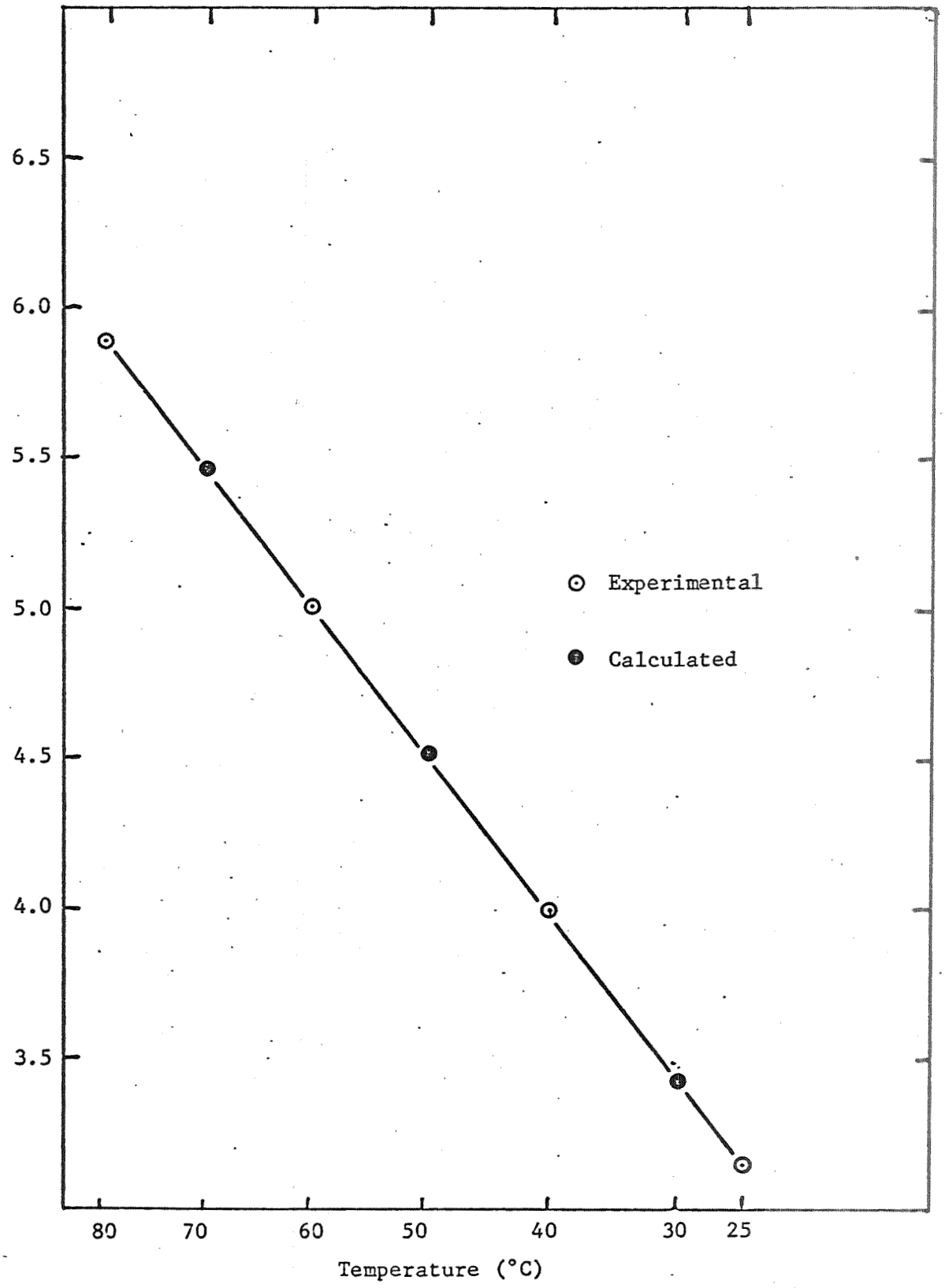

Figure 2.13. Temperature Dependence of "A" Coefficient

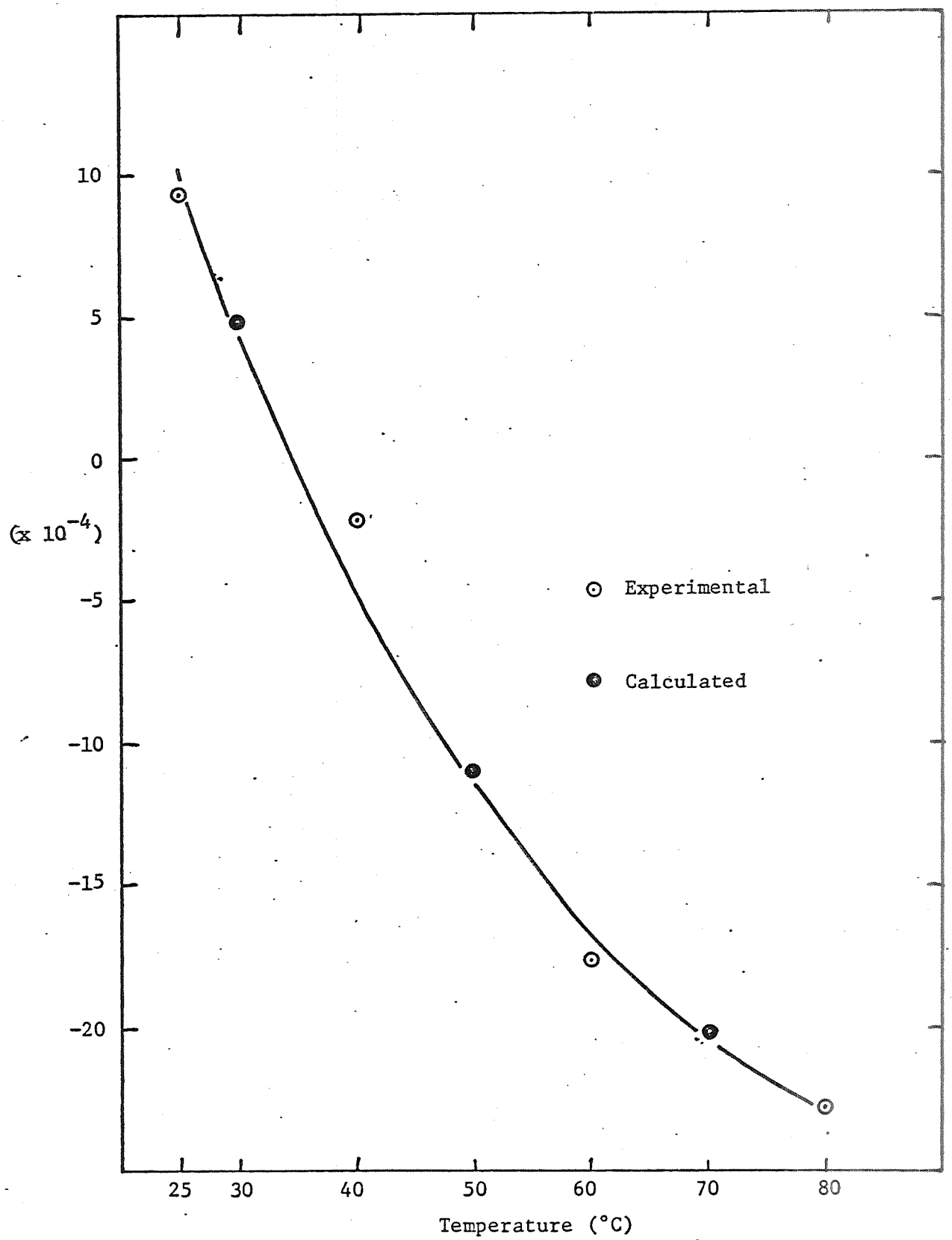

Figure 2.14. Temperature Dependence of "B" Coefficient

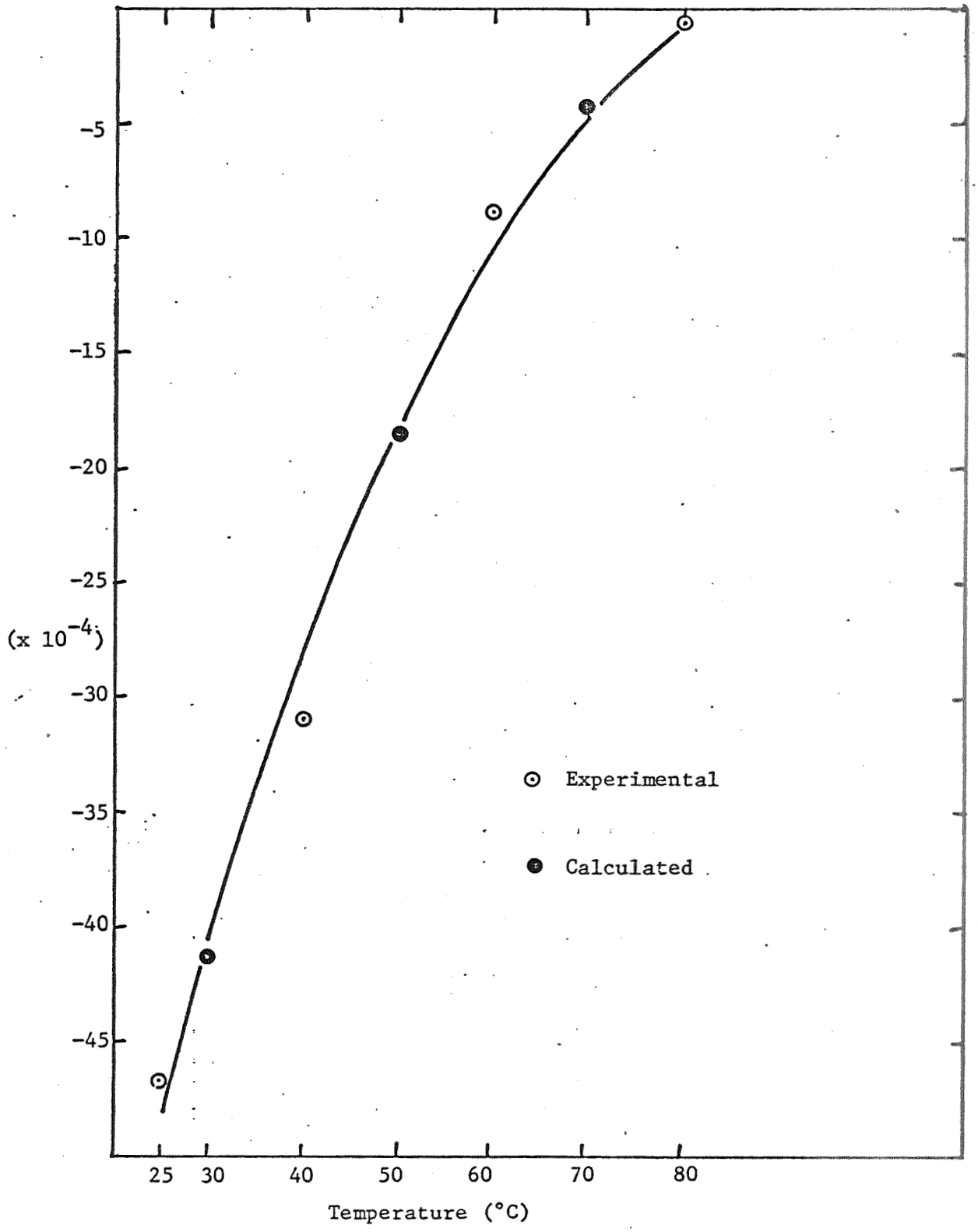

Figure 2.15. Temperature Dependence of "C" Coefficient

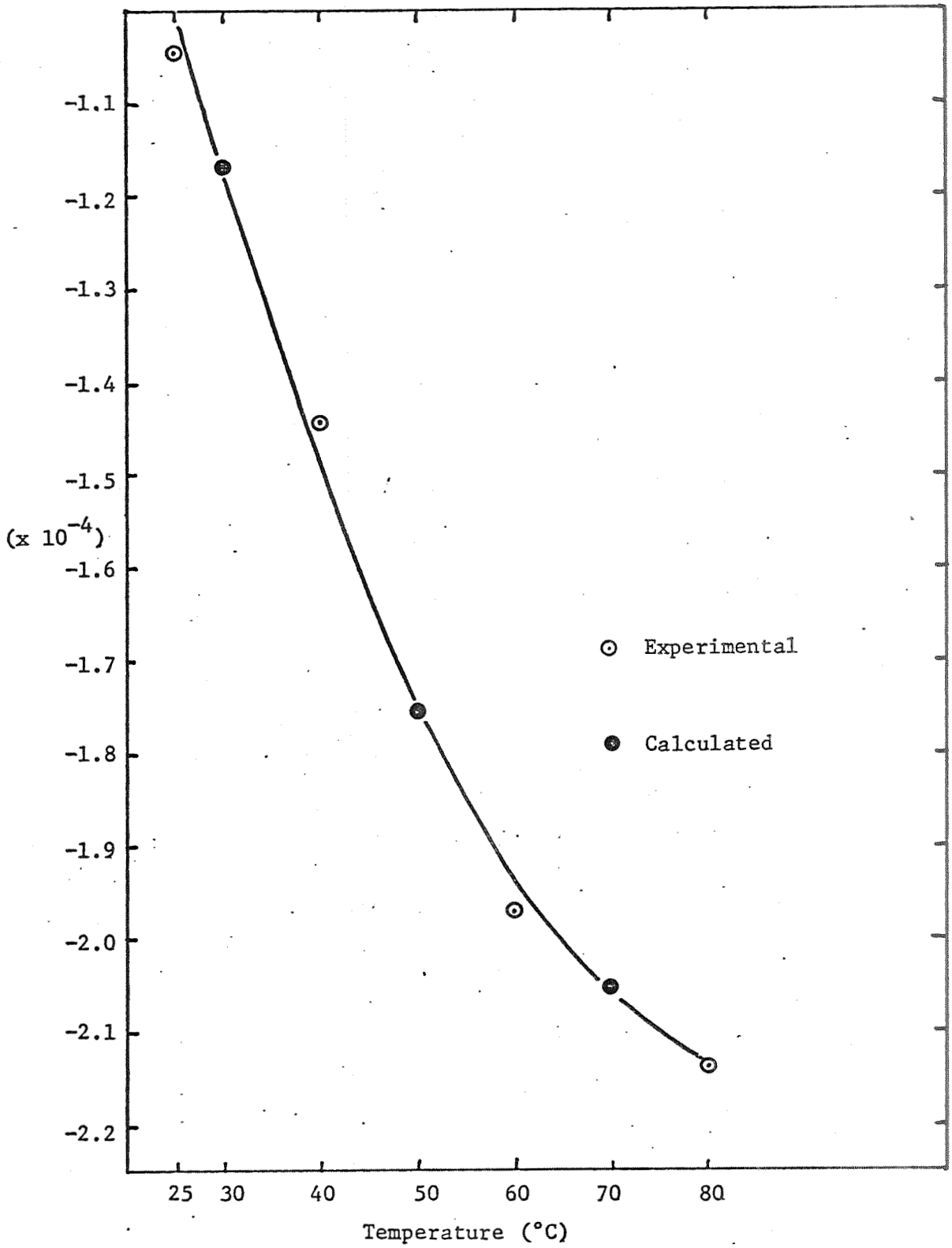

Figure 2.16. Temperature Dependence of "D" Coefficient

Table 2.7: Values of Coefficients Used to Fit Temperature Dependence of Original Coefficients

A_1	A_2	A_3
18.43276	-3721.606	-249768.9
B_1	B_2	B_3
1.089235	6.166202×10^{-3}	8.543493×10^{-6}
C_1	C_2	C_3
-0.1456833	7.980272×10^{-4}	-1.092004×10^{-6}
D_1	D_2	D_3
3.797876×10^{-3}	-2.236866×10^{-5}	3.117425×10^{-8}

equations which fit the temperature dependence of the vapor pressure of each individual solution. These points were then plotted versus total gram ions/1000 grams solution. They exhibited the same random scatter and were quite easily fitted to a cubic equation as were the original data points. These are shown in Figures 2.17 through 2.19. To add further credence to the method, the coefficients of

$$\ell n\ P = A + BM + CM^2 + DM^3$$

exhibited the same temperature dependency as did the coefficients fit to the original data. They, in fact, deviated very little from the best fit line drawn to fit the original coefficients as shown in Figures 2.13 through 2.16. The circles represent coefficients from data points at 25°, 40°, 60° and 80°; while the darkened circles are coefficients from the calculated points at 30°, 50° and 70°. The line is the best of the original coefficients.

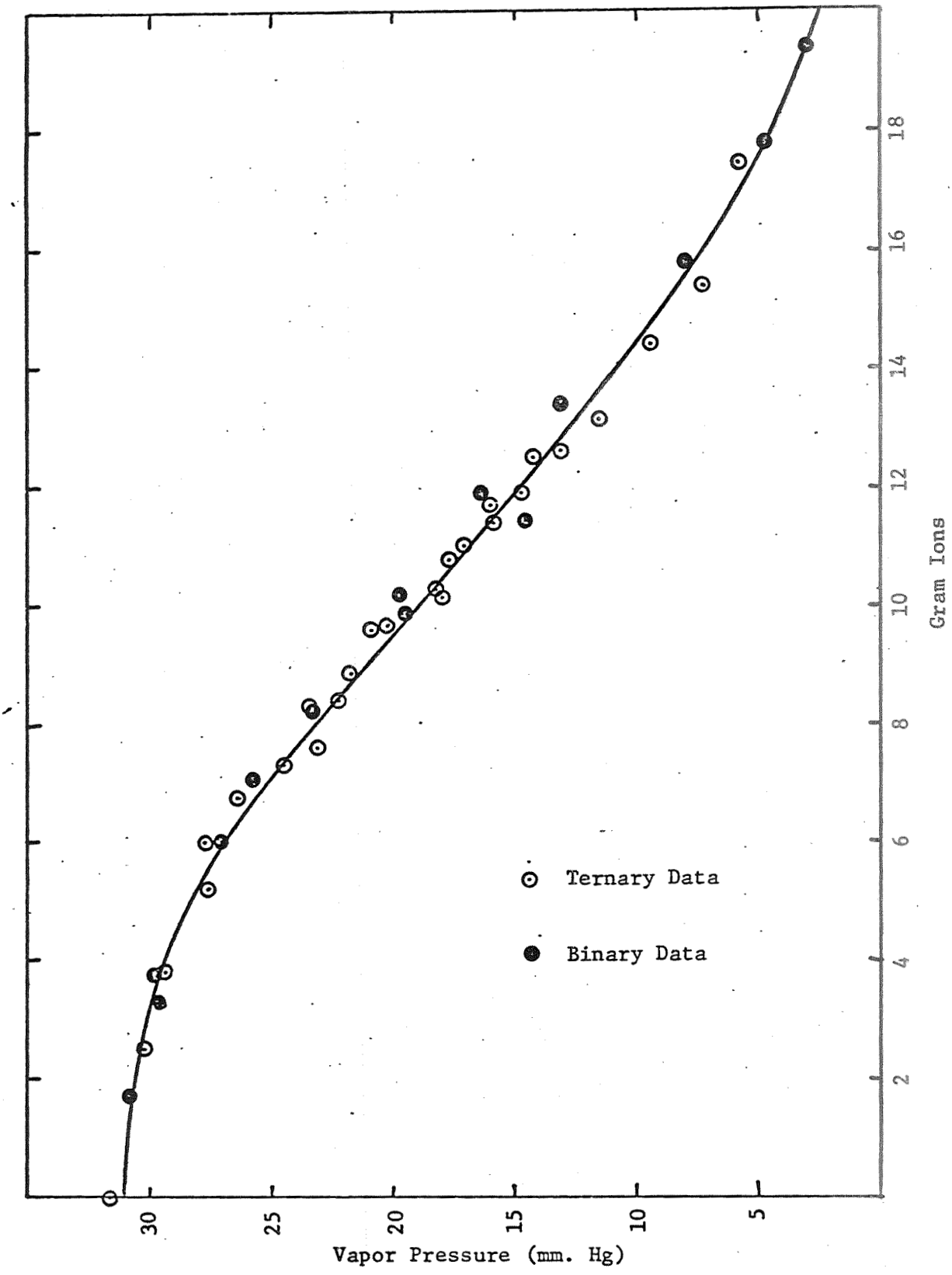

Figure 2.17. Concentration Dependence of Vapor Pressure at 30°C

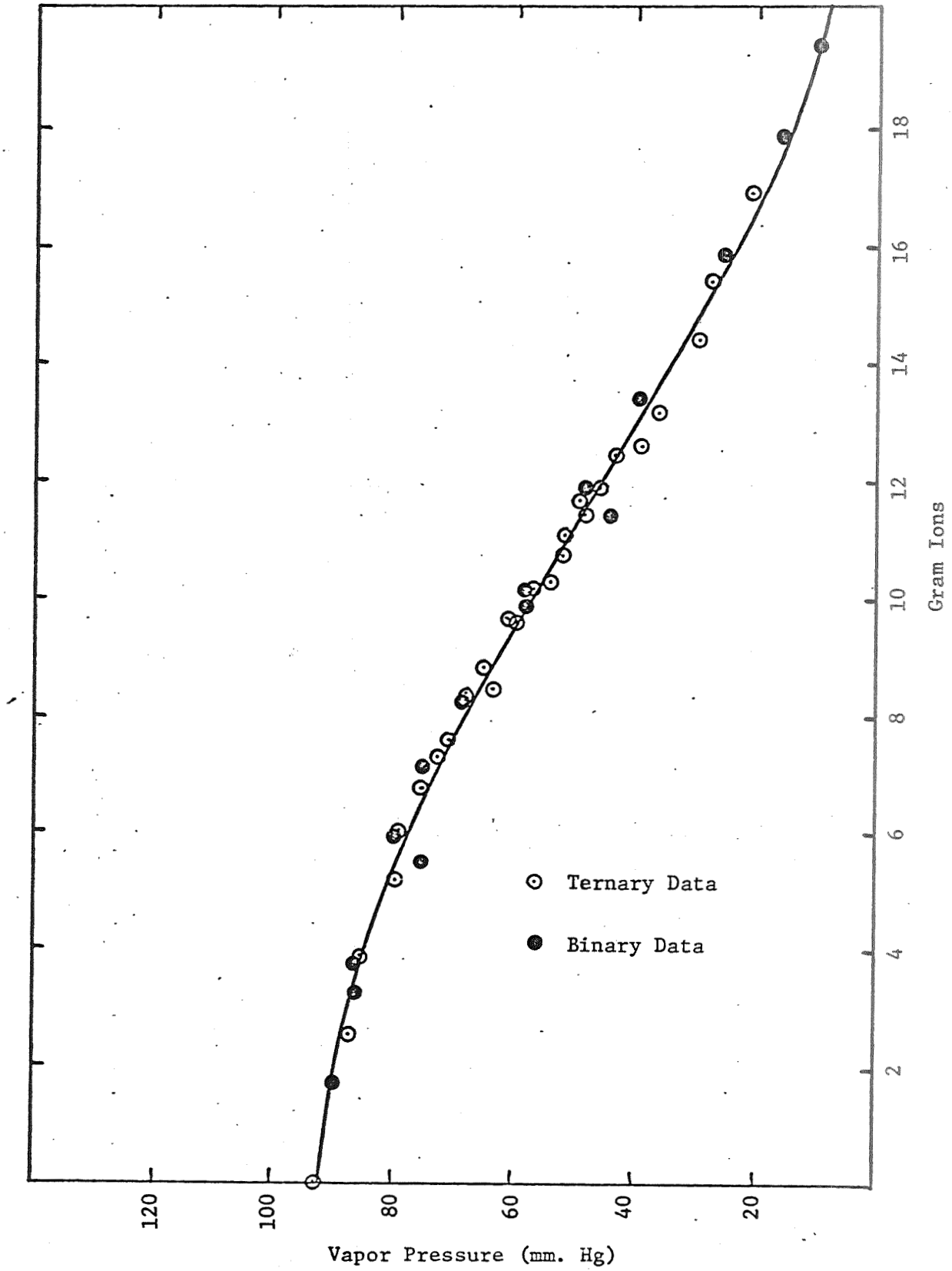

Figure 2.18. Concentration Dependence of Vapor Pressure at 50°C

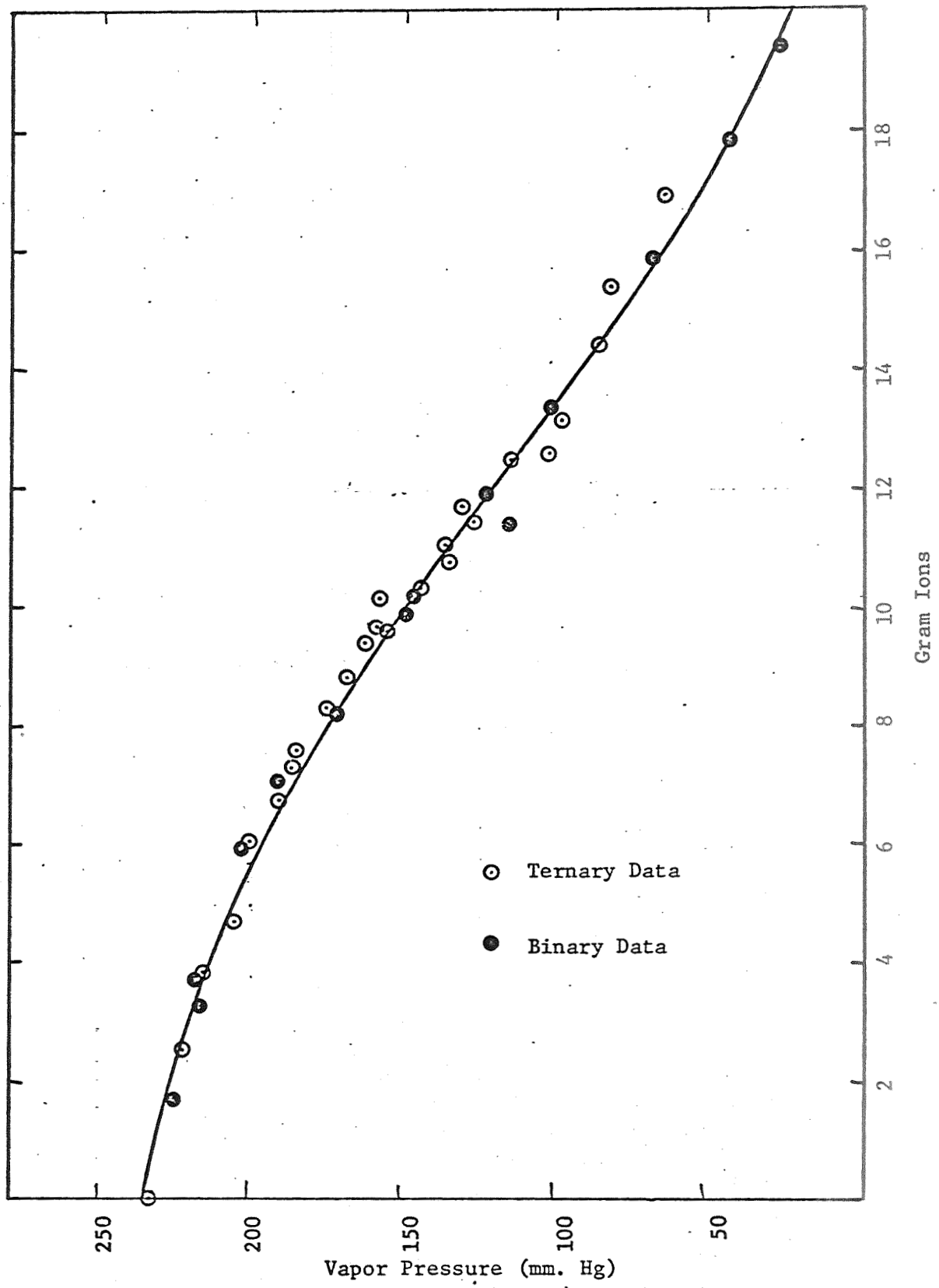

Figure 2.19. Concentration Dependence of Vapor Pressure at 70°C

2.5 Conclusion and Future Work

Future work in this field should consist of studying vapor pressure data for more systems. Some of this data will be available in the literature, some will have to be obtained experimentally. In this way extensions of the present work may result.

The most important question is whether or not other systems may be fitted by this same general form of equation. This is dependent on an even more fundamental question; i.e., are all ions sufficiently alike to produce the same kind of influence on vapor pressure and other thermodynamic properties. If they are not alike, then do the coefficients used to fit the data have any significance on the molecular level?

This method allows the fitting of strong ternary electrolyte vapor pressures from data for only one binary. For some systems it may be necessary to have data for both binaries or at worst for a few ternary points. For the $KOH-K_2CO_3-H_2O$ system all that is necessary at the temperatures in question are the vapor pressure data from one binary system ($KOH-H_2O$).

The basic postulate of this method is that all ions in the system (K^+, $CO_3^=$, OH^-) have the same effect on vapor pressure. This neglects the effect of ionic size, charge, and interactions with water. Whether or not these effects become more important at higher temperatures should be ascertained. It is suspected that they will have an appreciable effect.

This method should also be capable of predicting the behavior of more complicated systems; i.e., those containing more than three kinds of ions. Certain methods have employed total molality but these have never been accurate for the highly concentrated solutions in question here. However, very few data exist for more complicated systems, either ternary systems with four distinct ions, or quaternary systems.

One procedure for data correlation which could prove to be a simplification of the procedure used here remains to be investigated. Fitting $1 - P/P_o$ vs. the concentration variable (where P is the vapor pressure of the solution and P_o that of water) gives the same type of curves obtained in this analysis. The temperature-dependence of the coefficients thus obtained could not be ascertained. Perhaps it would be possible to obtain an analytical form in which the coefficients are not temperature-dependent. If, in fact, all ions exert the same influence at these temperatures, this would give a general equation for vapor pressures of solutions of nonvolatile electrolytes.

A new manometer is in the design stage. It will have a much larger range (in the vicinity of 300 mm) and will be constructed of metal. Measurements will be made by electrical contacts rather than by visual means. This should improve accuracy by eliminating the use of standard solutions. The problem of deposits on the mercury surface which do not permit accurate visual sighting should also be eliminated. Metal will also allow high temperature measurements to be made more easily.

3. Partial Molal Volumes of Gases Dissolved in Electrolyte Solutions

The experimental determinations of the partial molal volume of gases in water and various electrolyte solutions is now essentially complete. Studies have been made of the KOH system, other salting-out electrolytes, and some salting-in salts. The experiments were designed to study the effect of ionic size and charge; ion concentration; and ion type on the partial molal volumes of various solute gases in these electrolyte solutions. In section 3.1 a brief review of previous experiments is given and in section 3.2 a detailed description of the experimental apparatus and method is presented. The results of experiments with gases in various electrolyte solutions are given in section 3.3 and a comparison with the previously described[6] theory is made in section 3.4.

3.1 Introduction

There has been no comprehensive study made of the partial molal volume of nonpolar gases in ionic solutions. A few scattered data exist, e.g., oxygen in sea water[7], and nitrogen and methane in sodium chloride[8]. Both of these studies report values obtained from high pressure solubility measurements. There have been a number of studies of the partial molal volume of gases in pure water. Ångström[9,10] was the first to measure dilatometrically the change in solution volume upon the dissolution of a series of slightly soluble gases in pure water. The comprehensive studies of Horiuti[11] did not include

any studies in water and it was not until the 1945 work of Kritchevsky and Ilinskaya[12] that any other partial molal volumes of gases in water appeared. Since then there have appeared several other studies in water by high pressure solubility measurements[7,8,13,14] and densitometry[9,13]. While most of these data are consistent to about 8%, discrepancies as high as 30% are common. The primary reason for this variation is the extremely low solubility of most gases in water.

The aim of this experimental study was to determine the effect of ionic concentration, ion species, and molecular properties of the solute gas on the partial molal volume of the solute in an electrolyte solution. Two broad categories of salts were used in this study: salting-out electrolytes such as the alkali halides and potassium hydroxide, and salting-in electrolytes such as the tetra-alkyl ammonium bromides. The alkali halides were used because of their well-defined solution behavior and the potassium hydroxide system was studied because of its importance as a fuel cell electrolyte. The tetra-alkyl ammonium salts were studied because of their peculiar solution behavior (e.g., large salting-in effects[15,16,17], high viscosity[18,19] unusual molal heat capacity[20,21], and activity coefficients[22,23]). It is quite possible that these types of ions might have valuable practical significance in improving the solubility of some solutes. This could be of industrial significance in certain stagewise separation processes where the use of ionic additives or mixed electrolyte solutions could be used to adjust salting-in or salting-out characteristics as well as other thermodynamic properties. The

possible use of mixed electrolytes in fuel cells is another area of particular interest that has not as yet been studied thoroughly.

The effects of ionic radii were studied by measuring the partial molal volume of argon in KCl and KI, and of argon and methane in $(CH_3)_4NBr$ and $(C_4H_9)_4NBr$. The effect of the solute gas properties was studied by measuring the partial molal volumes of argon, methane and ethane in KCl solutions. In the salting-in systems the gases argon and methane were used. The effect of ionic charge was studied by measuring argon in $CaCl_2$. The strongly salting-out system KOH, in particular the O_2-KOH and H_2-KOH systems were studied for their special significance to fuel cell operation. All of the partial molal volumes determined in this study were at atmospheric pressure and 25°C.

3.2 Apparatus and Experimental Procedure

At low pressures (atmospheric) two distinct techniques to determine the partial molal volume of slightly soluble gases in liquid solutions have been used: these are Horiuti's dilatometric method[11], and sensitive solution density determinations[13,24]. The latter method needs extremely good temperature control as well as a method for measuring relative solution densities to an accuracy of 10^{-7} (10^{-8} for concentrated electrolyte solutions). Another method to determine the partial molal volume is high pressure solubility studies. If one determines the solubility over a suitable range of pressure, the partial molal volume can be determined from the relation

$$\bar{V}_i - \bar{V}_i^0 = RT \left(\frac{\partial \ln \gamma_i}{\partial P} \right)_{T,n_{j\neq i}} \qquad (3\text{-}1)$$

Taking slopes of such solubility-pressure plots often involves a large percent error and such measurements were generally considered unsuitable for the electrolyte solutions studied in this work. It is generally felt that the Horiuti dilatometric method is the best of these, and it is used by most workers in the field[25]. We have used a modification of the Horiuti method in this work. Most dilatometric measurements have been done on systems where the mole fraction solubility of the solute gas was about 10^{-2} - 10^{-4}. The systems encountered in this study had considerably lower solubilities, $x_1 \sim 10^{-5}$ - 10^{-6}, and an increase in the size of the dilatometer as well as extremely accurate temperature and pressure controls were required in order to achieve the desired $\bar{V}_i$ measurements of gases in ionic solutions.

3.2.1 Experimental Apparatus

The experimental apparatus is essentially that of Horiuti[11] with a few important improvements. Figure 3.1 shows the modified dilatometer in which the actual partial molal volume measurement is made. It is constructed entirely out of glass and consists of a 500 ml bulb with calibrated precision bore capillary side arms and an externally driven magnetic stirring device. One of the capillary side arms is fused inside the lower portion of the bulb for the purpose of passing gaseous solutes directly into the solution liquid. Mercury in the bottom of the dilatometer serves to isolate the solvent in the bulb and also indicates the total system volume by the position of the mercury threads in the capillary side arms. Sealed into the bulb is an all-glass enclosed magnetic bar attached to a stirring shaft with

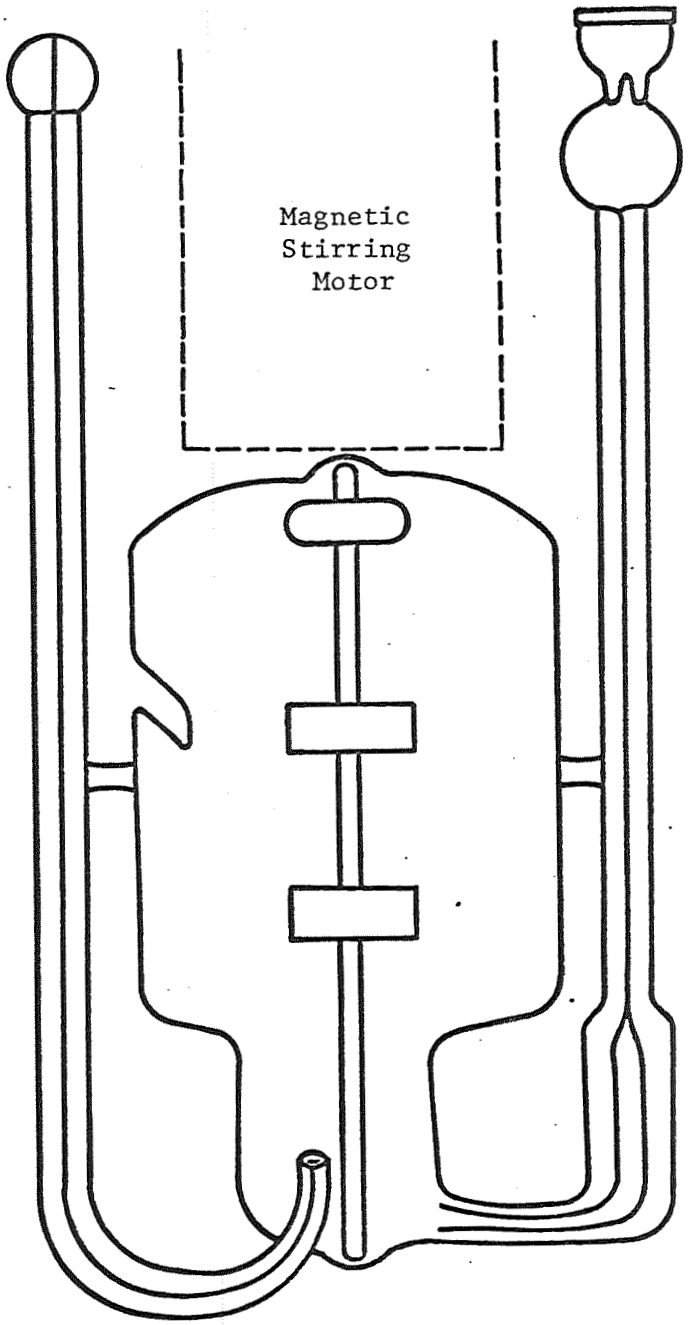

Figure 3.1. Dilatometer in Which the Measurement of the Partial Molal Volume is Made.

blades that can be driven by an external magnetic motor. The dilatometer bulb is of much greater volume than used by Horiuti (40-150 cc), principally bacause the gas solubilities encountered in concentrated electrolyte solutions are usually about an order of magnitude or more smaller than those in pure water. Table 3.1 shows the various sizes of dilatometers used in this study. The capillary side arms of the dilatometer were made of Trubore capillary tubing and calibrated by introducing a known weight of very pure mercury into the capillary thread and after equilibration in the constant temperature bath reading the volume of the mercury with a cathetometer.

The entire system is shown schematically in Figure 3.2. The dilatometer is placed in a commercially available constant temperature bath, the Neslab Model TEV70, equipped with quartz infra-red heaters and solid state relays having a very rapid response time. A circulating cooling system, Neslab Model RTE3, was used in conjunction with the main bath in order to achieve the desired temperature control of $\pm$ 0.001°C at 25°C. The temperature was monitored with a Hewlett-Packard quartz thermometer capable of a digital temperature display with a resolution of 0.0001°C. Two temperature sensing probes were used; one in the bath itself and another which could be placed in a temperature sensor well in the dilatometer. This instrument allowed us to monitor the temperature of the system at will and aided in establishing good overall temperature control (i.e., $\pm$ 0.001°C). The temperature control system was stable for a few days provided there were no drastic environmental fluctuations. If the room temperature changed appreciably a resultant drift of a few thousandths of a degree in the bath temperature was noted.

Table 3.1: Calibration of Dilatometers

Dilatometer Number	Approximate Total Volume of Dilatometer CF.	Capillary Side Arm I.D. (± 0.001) m.m.
1	500	0.513
2	500	0.762
3	500	0.689
4	500	0.768
5	500	0.500

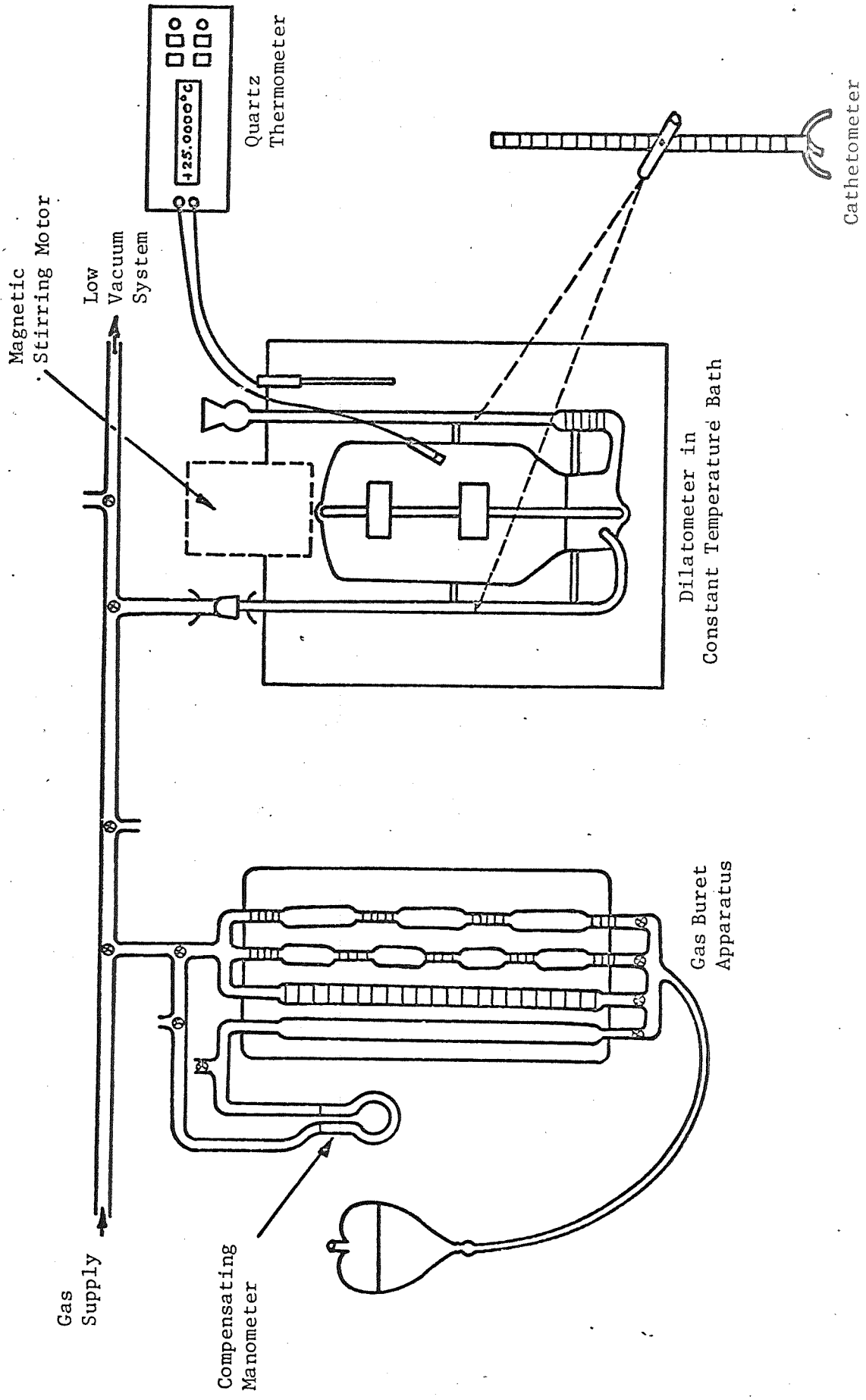

Figure 3.2. Schematic Diagram of Partial Molal Volume Apparatus.

Since the temperature had to be controlled accurately only at the start and end of an experiment, any temperature shifts during a run could be accounted for by simply shifting the temperature control set-point slightly until the system was again stable at the initial temperature. In this way the system temperature initially and finally was constant ($\pm$ 0.001°C) and no temperature induced volume correction was required. Although the bath temperature had instantaneous random fluctuations of $\pm$ 0.001°C it was estimated that for most runs the temperature fluctuations inside the dilatometer were somewhat less.

A gas buret, consisting of a series of calibrated bulbs of about 2cc and 5cc volume (see Table 3.2) and a 5cc precision microburette, which was housed in a plexiglas box, was connected to the dilatometer in the bath. A compensating manometer filled with a sensitive (S.G. = 1.75) indicating fluid enabled one to measure gas volumes to an accuracy of $\pm$ 0.002 ml. All tubing connecting the gas buret to the dilatometer was capillary tubing to minimize the volume and all stopcocks were precision bore pressure stopcocks to eliminate any leakage of gas as it is transferred from the buret to the dilatometer. Volume changes were read by a cathetometer situated about 5 feet from the main bath. A barometer was also housed in the laboratory and enabled accurate atmospheric pressures to be determined.

3.2.2 Filling of Dilatometers

The dilatometers were carefully cleaned and charged with about 10cc of freshly cleaned pure mercury. It is extremely important that the dilatometer, mercury and electrolyte solution be clean and free from contaminants as the accuracy of the experiment can be drastically

Table 3.2: Calibration of Gas Buret Bulbs

Bulb	Volume, cc (± 0.001)	Volume of Capillary Lines Connecting the Gas Bulbs/Division
1A	--	--
2A	2.192	0.001
3A	2.289	0.001
4A	1.912	0.001
5A	1.983	0.001
1B	4.403	0.0009
2B	4.764	0.0009
3B	4.529	0.0009

affected by impure mercury surfaces in any dilatometer capillary lines. The solvent (in this case electrolyte solution) was initially filtered and then degassed by boiling under vacuum at room temperature in a 2 liter flask as shown in Figure 3.3. It is not as important to obtain a completely gas-free solvent as it is in solubility determinations since it is only necessary to determine solution volume changes due to incremental additions of the gas to the solution. It is advantageous, however, to have a well-degassed solvent since more gas can be dissolved in it, and in the case of concentrated electrolyte solutions this is very important owing to the extremely low gas solubilities. The dilatometer was connected to the degassing apparatus (as shown in Figure 3.3) and initially evacuated. The degassed solvent was then sprayed into the evacuated dilatometer through one of the capillary lines until it completely filled the bulb and side arms. Once filled the whole system was brought to atmospheric pressure, the dilatometer was disconnected from the degassing apparatus and turned upright. It was then placed in the constant temperature bath and the side arms emptied of their liquid content by forcing the mercury thread up along each stem. Mercury additions could be made so that the thread was situated in the calibrated section of the capillary side arms. Care was also taken to assure that there were no bubbles of gas in the dilatometer and that the mercury threads were unbroken and moved evenly in the capillary lines.

3.2.3 Measurement of Partial Molal Volume of Gases in Electrolyte Solutions

The charged dilatometers were allowed to equilibrate in the bath for several hours with constant stirring. The capillary lines

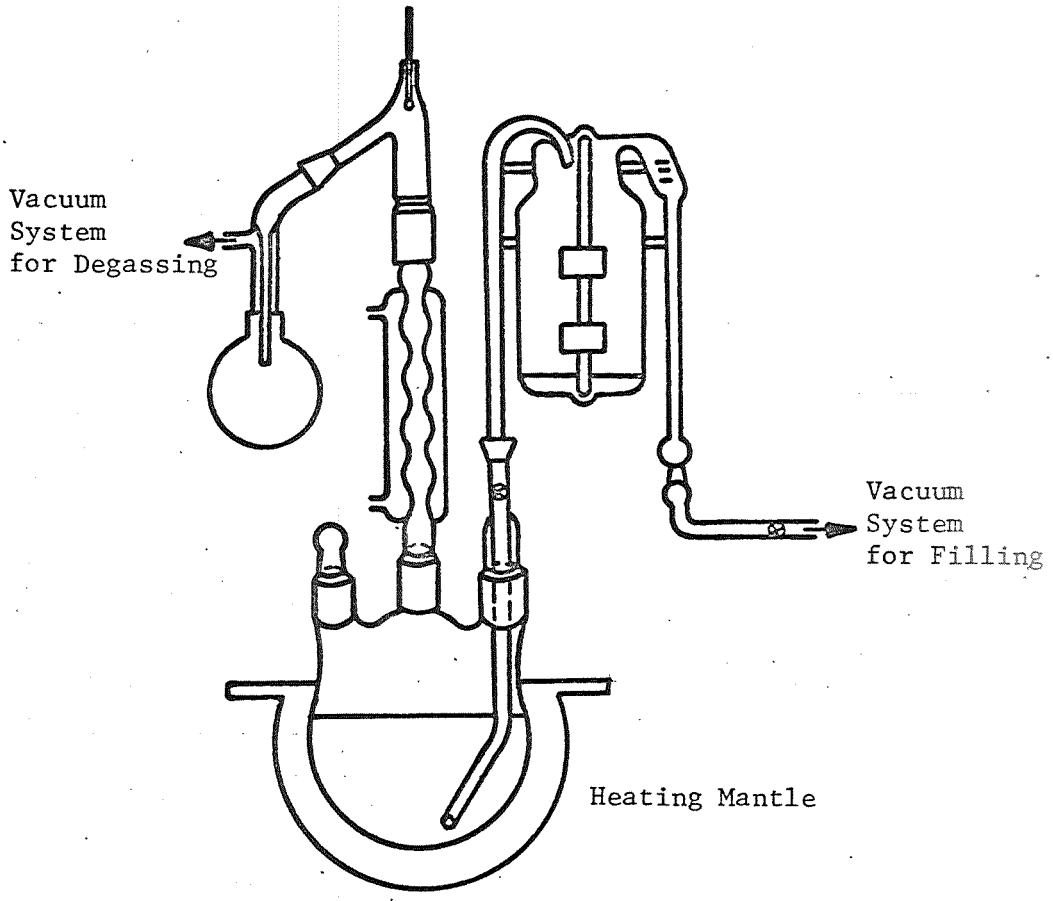

Figure 3.3. Apparatus for Degassing Electrolyte Solutions and Filling of the Dilatometer.

leading into the dilatometer and from the gas buret were flushed with the solute gas and then connected to the gas buret. The whole system, dilatometer and gas buret, was brought to atmospheric pressure and the volume of gas and the heights of the mercury threads in the dilatometer were read. Bath temperature, gas temperature and barometric pressure were also noted. The desired volume of gas (0.5-3.0cc) from the gas buret was allowed to bubble into the dilatometer under pressure from the mercury leveling tube and/or a low suction applied to the atmospheric leg of the dilatometer. After passing the desired amount of gas into the dilatometer the gas buret was brought back to the reference pressure conditions by means of the compensating manometer and the final gas volume was noted. A correction was made for the change of height of the mercury thread in the dilatometer and this volume was added to the reading obtained from the gas buret.

Even with constant stirring,the dissolution of the gas required anywhere from several hours in pure water to a full day or more in some of the concentrated electrolyte solutions. Great care was taken to insure that all gas was dissolved and that there were no residual small bubbles of gas trapped in the mercury. If, after complete dissolution of the gas, the bath temperature had fluctuated more than 0.001°C from the initial value it was brought back to the original temperature by an adjustment of the controller set-point to eliminate any volume changes due to temperature variations. Compressibility effects due to the additional pressure caused by a rise in the height of the mercury threads after complete dissolution of the gas had to be accounted for. In order to avoid any corrections, the pressure inside the dilatometer

before gas addition and after complete gas dissolution had to be the same. This was accomplished by pulling a slight suction on one of the legs of the dilatometer so that the height of mercury in the other, the atmospheric side, returned to its original (before gas addition) level. The volume change of the system was then read with the cathetometer by noting the change in heights of the mercury threads. This compressibility correction was one of the major sources of error in earlier $\bar{V}_i$ work and the method described here is an effective and correct means of avoiding any compressibility corrections due to pressure change. Atmospheric pressure changes were usually not significant during a run; however, the barometer was read again at the end of a run and a correction was possible when a significant change in barometric pressure occurred.

Depending upon the gas solubility one to four additions of gas were made to the same solution. From the definition of the partial molal volume

$$\bar{V}_i = \left(\frac{\partial V}{\partial n_i} \right)_{P,T,n_j} \approx \left(\frac{\Delta V}{\Delta n_i} \right)_{P,T,n_j} \qquad (3\text{-}2)$$

incremental changes of volume resultant from incremental changes of gas added to the solution gives $\bar{V}_i$. All of the solutions encountered were extremely dilute (about 10^{-5} moles of gas added) so that the partial molal volumes so determined were the limiting values for an infinitely dilute solution of gas in an electrolyte solution.

3.2.4 Chemicals and Preparation of Solutions

Argon, hydrogen and oxygen were 99.9% min. purity supplied by

Airco, and methane and ethane were C.P. grade 99.0% min. purity supplied by Matheson Gas Products. KCl, KI, KOH and $CaCl_2$ were Baker Analyzed Reagent Grade, and the tetra-alkyl ammonium bromides were C.P. grade supplied by Eastman Kodak Chemicals Company. All of these salts were used without further purification. Electrolyte solutions were prepared by dissolving weighed quantities of the salts in distilled water. The resultant solutions were filtered before analysis. The solutions were analyzed after degassing by titrating with a standard silver nitrate solution. A check of some of the solutions after the experiment showed that no significant concentration changes occurred due to handling of the electrolyte solution during any run.

3.2.5 Special Precautions

Other than care in cleaning of dilatometer, mercury and solution, and stringent temperature control, there are a few additional precautions to note. Most important is the fact that minute gas bubbles can become trapped in the mercury and if these are not completely dissolved will give erroneous total volumes readings. These bubbles may be avoided if the stirring is stopped at the time of gas introduction. The gas then tends to remain in large bubbles and does not break up into small bubbles which might be trapped in the mercury. Another problem has been the phenomenon of creeping of the solution in the capillary lines. This makes itself manifest especially in the tetra-alkyl ammonium systems and in systems where the gas dissolution is very slow. It is evidenced by a small layer of solution that appears over the mercury thread. In reading the final volumes these increments of solution must be included

in the total volume to insure an accurate reading. This problem was alleviated by being careful to dry the capillary threads initially and introducing dry mercury into the capillary just prior to the experiment. Additional problems were experienced with the KOH systems due to the etching of glass surfaces by concentrated KOH solutions. This meant that calibration of the dilatometer capillary legs was necessary after runs with concentrated KOH solutions, especially if the experiment required a long time (more than a day).

3.2.6 Calculations

The partial molal volumes of a gas in a solution was calculated as follows: A known volume of gas at a given temperature and pressure was charged into a solvent filled dilatometer. The number of moles, Δn, of gas added was calculated from a virial equation of state

$$\frac{Pv}{RT} = 1 + \frac{B(T)}{v} + \cdots \qquad (3\text{-}3)$$

using the first two virial coefficients. At room temperature this gives accurate results for all the gases used. Table 3.3 shows the values of B(T) at 300°K used in this study which were taken from Dymond and Smith[44]. The values of solution volume change were obtained by measuring the heights of the mercury thread before and after dissolution of the known amount, Δn, of the given gas. Knowing the values of the capillary diameter (Table 3.3) a volume change, ΔV, was determined. Having determined Δn and ΔV the partial molal volumes were calculated using Equation (3-2).

3.3 Results and Discussion

The experimental results for the gas-electrolyte solution systems studied are shown in Figures 3.4-3.7 and Tables 3.4-3.7. The deviations

Table 3.3: Second Virial Coefficients of Gases at 300°K

Gas	B(T) (cc/g mole)
H_2	15.0
O_2	-15.5
Ar	-15.6
CH_4	-42.0
C_2H_6	-18.3

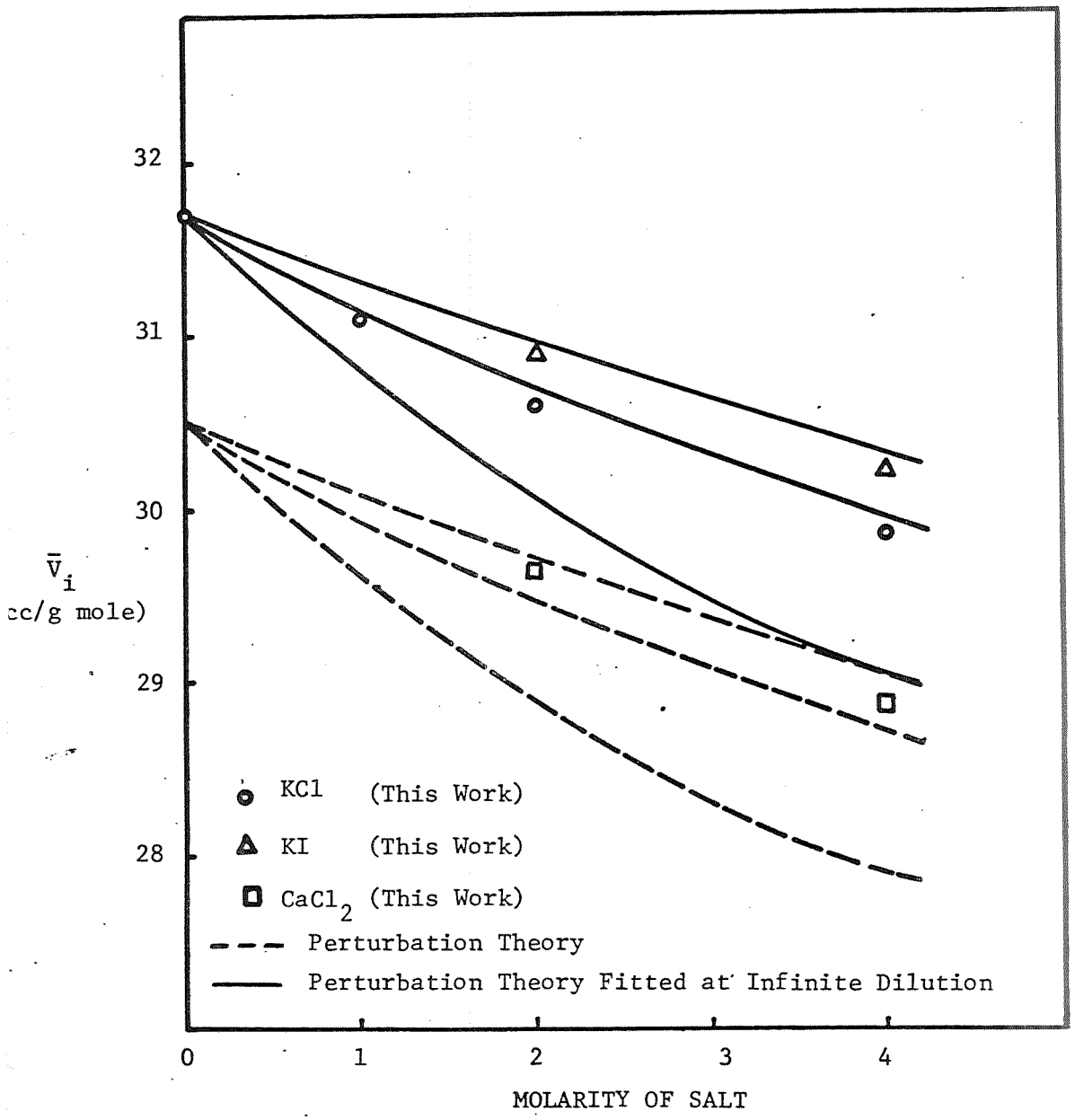

Figure 3.4. Partial Molal Volume of Argon in Electrolyte Solutions: Effect of Ionic Size and Charge.

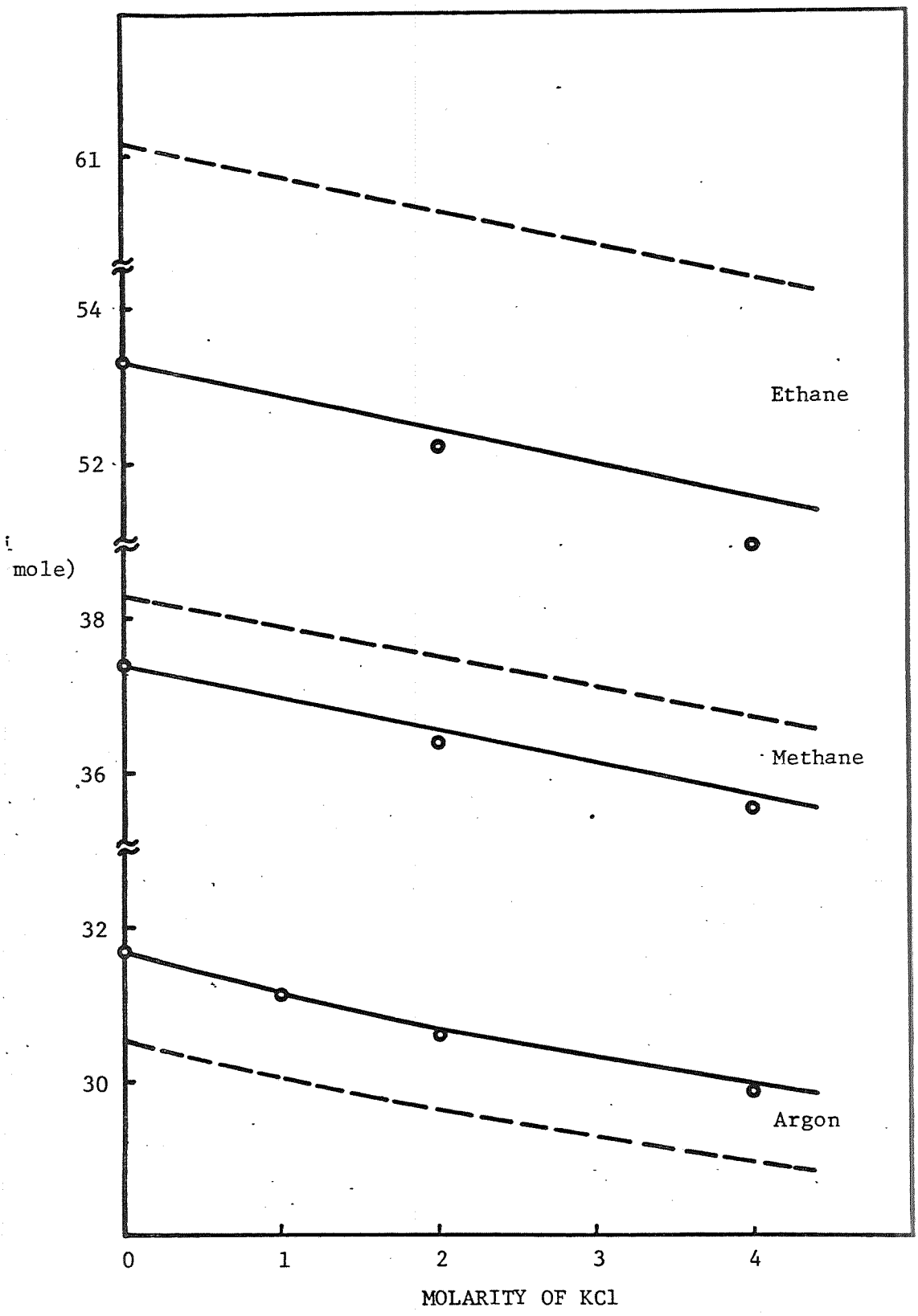

Figure 3.5. Partial Molal Volume of Various Solute Gases in KCl: Effect of Solute Size.

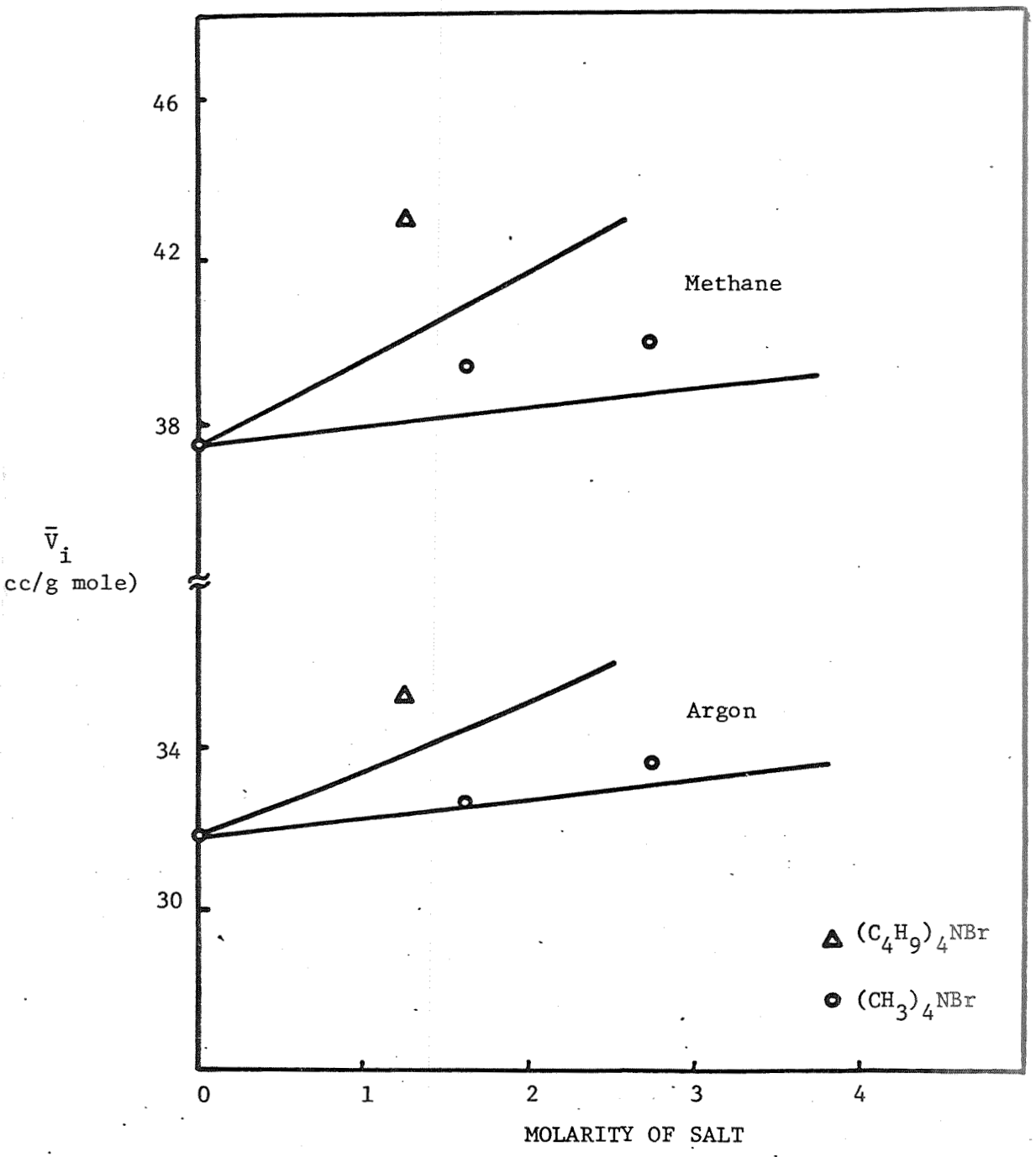

Figure 3.6. Partial Molal Volume of Ar and CH_4 in Salting-In Systems.

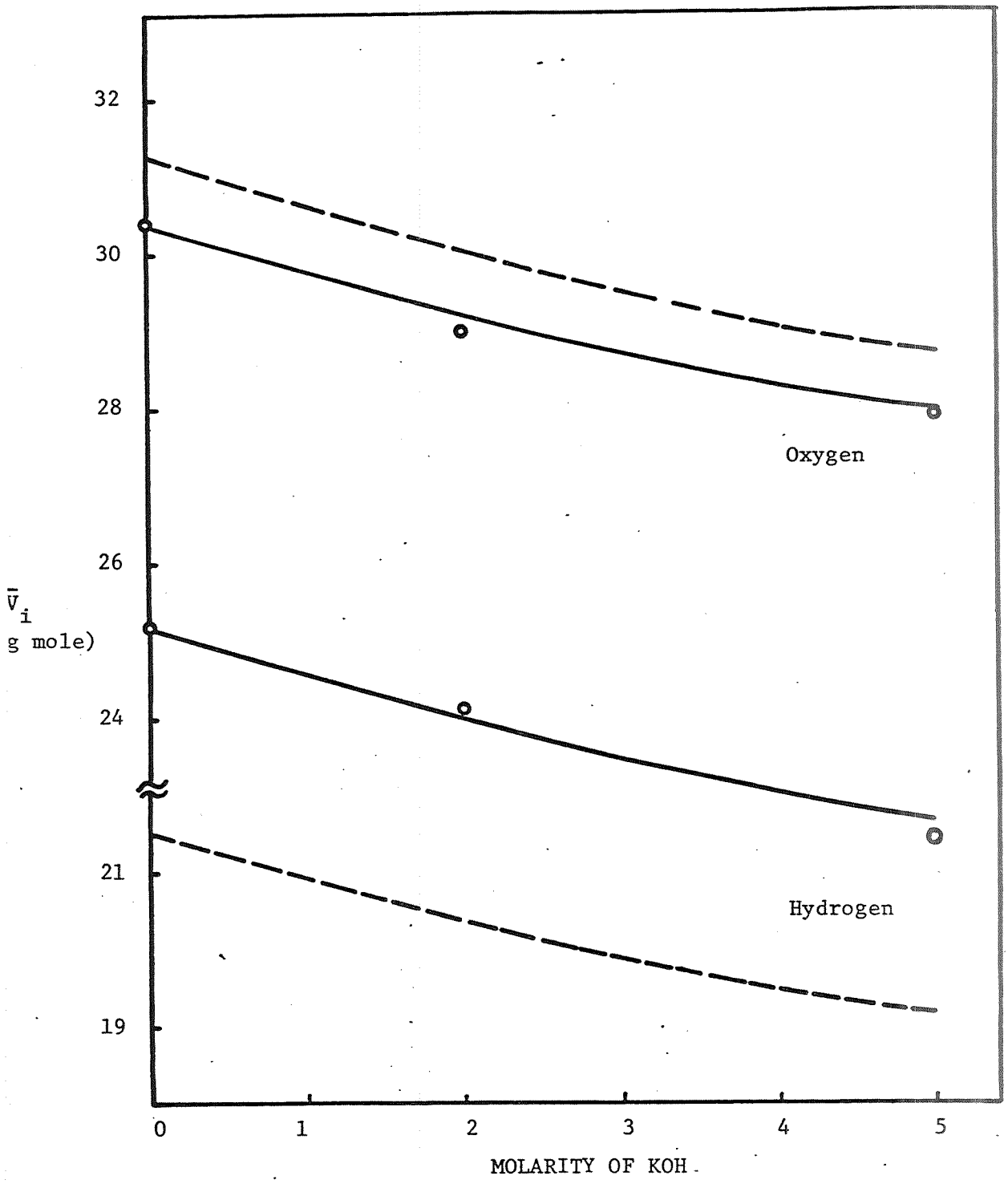

Figure 3.7. Partial Molal Volume of O_2 and H_2 in KOH Solutions.

Table 3.4: Partial Molal Volume of Argon In Various Ionic Solutions

25°C

Electrolyte	C	$\bar{V}_i$
	(g mole/ℓ)	(cc/g mole)
Water	0.0	31.71 ± 0.43
KCl	1.0	31.11 ± 0.64
KCl	2.0	30.60 ± 0.53
KCl	4.0	29.89 ± 0.83
KI	2.0	30.98 ± 0.47
KI	4.0	30.24 ± 0.42
$CaCl_2$	2.0	29.63 ± 0.79
$CaCl_2$	4.0	28.80 ± 1.42

Table 3.5: Partial Molal Volume of Gases in KCl at 25°C

Solute Gas	C	$\bar{V}_i$
	(g mole/ℓ)	(cc/g mole)
Ar	0.0	31.71 ± 0.43
Ar	1.0	31.11 ± 0.64
Ar	2.0	30.60 ± 0.53
Ar	4.0	29.89 ± 0.83
CH_4	0.0	37.42 ± 0.45
CH_4	2.0	36.37 ± 0.66
CH_4	4.0	35.51 ± 0.65
C_2H_6	0.0	53.27 ± 0.81
C_2H_6	2.0	52.18 ± 0.87
C_2H_6	4.0	50.91 ± 0.97

Table 3.6: Partial Molal Volume of Argon and Methane in Tetra-Alkyl Ammonium Bromides

25°C

Solute Gas	Electrolyte	C	$\bar{V}_i$
		(g mole/ℓ)	(cc/g mole)
Ar	Water	0.0	31.71 ± 0.43
Ar	$(Me)_4NBr$	1.62	32.64 ± 0.77
Ar	$(Me)_4NBr$	2.74	33.76 ± 0.77
Ar	$(Bu)_4NBr$	1.25	35.37 ± 0.86
CH_4	Water	0.0	37.42 ± 0.45
CH_4	$(Me)_4NBr$	1.62	39.39 ± 1.57
CH_4	$(Me)_4NBr$	2.74	39.99 ± 1.50
CH_4	$(Bu)_4NBr$	1.25	43.04 ± 1.22

Table 3.7: Partial Molal Volume of Hydrogen and Oxygen in Potassium Hydroxide

Solutions at 25°C

Solute Gas	C	$\bar{V}_i$
	(g mole/ℓ)	(cc/g mole)
O_2	0.0	30.38 ± 0.97
O_2	2.0	29.01 ± 0.56
O_2	5.0	27.97 ± 0.61
H_2	0.0	25.20 ± 0.56
H_2	2.0	24.09 ± 0.71
H_2	5.0	22.41 ± 1.33

shown in the tables are the standard deviations from the arithmetic mean of three or more experiments. The precision of the measurements is about $\pm$ 1.5% for gases in water and about $\pm$ 3% in ionic solutions. Most of the gas-pure water systems were estimated to have a total experimental error of about $\pm$ 3% while the concentrated electrolyte solutions errors are estimated at about $\pm$ 6%. The results of this work agree with most of the literature values for gases in pure water and the reproducibility of these experiments is about the same or somewhat better than most previously reported results. The primary source of these errors was the low solubility (~ 10^{-5} moles) of the gases in the solutions studied. This resulted in having to determine accurately volume changes as small as 10^{-3}cc. Temperature fluctuations were the primary source of error in making these volume measurements and pressure variations caused an additional error though very much smaller than the temperature effects. Even though the partial molal volumes were calculated by a finite differential approximation (Equation 3-2) the $\bar{V}_i$'s so calculated represent the partial molal volume at infinite dilution because of the very low mole fractions of gas in the ionic solution (~ 10^{-5} - 10^{-6}).

In Figure 3.4 the effect of various salts on the partial molal volume of argon is shown. It is first seen that for these salting-out ions the effect of increasing salt concentration decreases the partial molal volume although not drastically. For the salts KCl and KI the effect of increasing the size of one ion (I^- > Cl^-) tends to increase the partial molal volume at the same ionic concentration. This trend is again shown later for the salting-in systems. For the

salt $CaCl_2$ a more marked decrease is seen. It is difficult to say exactly whether the decrease in $\bar{V}_i$ is due simply to the ionic charge or to a combination of size effects ($K^+ > Ca^{++}$) and an increase in the number of ions present at a given concentration. It seems that the effect of ionic size is not very marked and certainly much of the decrease in $\bar{V}_i$ for the $CaCl_2$ system is due to the larger ionic charge.

In Figure 3.5 the effect of solute properties on the partial molal volume of a series of gases in KCl is shown. All gases showed a decrease in $\bar{V}_i$ with increasing ion concentration. Although this decrease appears to be slightly larger for increasing solute sizes ($C_2H_6 > CH_4 > Ar$) it is difficult to draw any concrete conclusions since the effects are quite small.

Salting-in systems are shown in Figure 3.6. The solute gases argon and methane were chosen because they have similar molecular properties yet these two gases show quite different solubility behavior in the tetra-alkyl ammonium salts[16,25]. It is seen that the partial molal volumes increase with ionic concentration as well as with ionic size. Evidence of this latter effect was already seen in the salting-out systems KCl and KI. The increase in solubility that argon undergoes in the series of salts KBr, $(CH_3)_4NBr$ and $(C_4H_9)_4NBr$ is, as was already mentioned, primarily a size effect. The increase of methane solubility in the same salts is somewhat different, however. In all of the tetra-alkyl ammonium salts the solubility of hydrocarbon gases such as methane increases much more rapidly than for any of the inert gases[16]. It seems that the addition of these types of ions in aqueous solution leads to a very specific interaction of the tetra-alkyl ammonium ions with the

hydrocarbon solutes. It has been suggested[16,26] that there exists a very definite nonelectrolyte-ion interaction which is a so-called "hydrophobic interaction." Other researchers[27-29] have as well concluded that certain hydrocarbon molecules form loose "hydrophobic bonds" with R_4N^+ ions and that the greater this attractive interaction the greater will be the solubility of that solute in the ionic solution. This effect is more pronounced for larger solutes. For example, the series methane, ethane, propane and butane shows increasing salting-in both with increases in the solute size as well as increases in the ion size; i.e., more salting-in as the size of R_4N^+ increases.

It is known[30-38] that the partial molal volume of gases is much larger in hydrocarbon solvents than it is in pure water. Table 3.8 shows this effect for several gases. The addition of the tetra-alkyl ammonium ions has the effect of making these aqueous solutions more "hydrocarbon-like"[16,29] and the resultant increase in this characteristic of the solution has resulted in a slight increase in the partial molal volume of these two gases in the salting-in systems.

The H_2-KOH and O_2-KOH systems are shown in Figure 3.7. The importance of these systems is in the study of fuel cell behavior as a function of pressure. The KOH system is a strong salting-out system and the partial molal volume of both hydrogen and oxygen show decreases with increasing salt concentration.

3.3.1 Comparison of Results

There are no reported results available for the partial molal volumes of gases in the ionic systems studied in this work. A comparison of the partial molal volume of gases in pure water is available, however,

Table 3.8: Partial Molal Volume of Gases in Various Solvents

Solvent	$\bar{V}_i$ (cc/g mole)			
	H_2	Ar	CH_4	C_2H_6
H_2O	26	32	37	53
CH_3OH	35	--	52	--
C_6H_6	35	45	56	72
$n\text{-}C_6H_{14}$	41	47	60	68

References: 12, 30-37

and is shown in Table 3.9. Most of the results in pure water are consistent with those obtained in these experiments to within the estimated experimental errors. This work has shown that the $\bar{V}_i$ of gases in salting-out systems decreases slightly with increasing ion concentration. The only verification of this experimental trend is the work of O'Sullivan and Smith[39] who report $\bar{V}_i$ measurements of nitrogen and methane in NaCl solutions. Their results showed a slight decrease of $\bar{V}_i$ for these two gases as the concentration of NaCl increased. Enns et al.[7] have also shown that the $\bar{V}_i$ of oxygen in sea water is slightly less than its value in pure water.

A comparison of the experimental results with the previously described perturbation theory is also made in Figures 3.4-3.7. As is seen, the theory predicts both the salting-in and salting-out behavior of most of the systems. The solid lines were theoretical predictions that resulted from fitting the theory at zero concentration (i.e., pure water) and the dashed lines are the theoretical results for both pure water and electrolyte solutions.

The only other theoretical results that this work can be compared with are the correlations of Lyckman et al.[40] who have devised an equation for predicting infinite dilution $\bar{V}_i$ in pure solvent systems. A comparison of experiment, the present perturbation theory and the correlation of Lyckman et al. is shown in Table 3.10. The results show that perturbation theory is as good as their correlation for most cases. It is impossible to extend such a correlation to ionic systems, however, and comparisons of the present theory for electrolyte solutions is therefore, not possible.

Table 3.9: Partial Molal Volume of Gases in Water

25°C

Solute Gas	$\bar{V}_i$ (cc/g mole)		
	This Work	Literature Value	Reference
Ar	31.7	32.2[a]	17
CH_4	37.4	36.9[b]	20
		37[c]	16
		37.1[a]	31
C_2H_6	53.3	51.0[b]	20
H_2	25.2	26[c]	16
O_2	30.4	32.1[a]	17
		31[c]	

Experimental Methods

a = High Pressure Solubility

b = Densitometry

c = Dilatometry

Table 3.10: Partial Molal Volumes of Gases in Water

Solute Gas	$\bar{V}_i$ (exp.)	$\bar{V}_i$ (this work)	$\bar{V}_i$ (Lyckman et al.)
		(cc/g mole)	
Ar	31.7	30.5	27.0
H_2	25.2	21.5	22.7
O_2	30.4	31.2	26.6
CH_4	37.4	38.2	34.9
C_2H_6	53.3	61.1	51.8

4. Diffusion Coefficients of Hydrogen in Lithium Hydroxide Solutions

Diffusion coefficients of hydrogen in 1-5 Normal lithium hydroxide solutions have been measured using the stagnant micro-electrode. The temperatures of measurement were 25, 40, 60 and 80°C. The dropping mercury electrode used previously was not suitable for this purpose due to the high hydrogen over-voltage on mercury electrode.

4.1 Materials

Pellets of lithium hydroxide with purity of 95.5% were used. Solutions were prepared from degassed, deionized distilled water.

Standard hydrochloric acid and potassium ferrocyanide solutions were prepared from ampules of Acculate Standard Solutions.

Potassium chloride used was of Analytical Reagent Grade.

4.2 Apparatus

The apparatus used in this experiment has been discussed in detail previously[41]. Only minor changes where made in the present set up. The microelectrode was made from standard taper joint with precision bore capillary. The platinum disc was cemented to the end of the male joint using fluorocarbon epoxy cement. To prevent freezing of the male to the female joint teflon sleeves were used. To prevent electrical leaks, the wire connecting the counter electrode was insulated with nylon tubing.

4.3 Calibration of Microelectrode Area

Calibrations of the microelectrodes were made using 0.005 M

potassium ferrocyanide solutions. This system gives high reproducibility, and handling of the solution is easily done. Moreover, at this low concentration, the diffusion coefficient can be considered as differential diffusion coefficient; hence, it is an ideal system for calibration purposes. The voltage used for all the calibration was + 0.7 volts. Three electrodes were calibrated; their areas were found to be 0.0270 cm^2, 0.025 cm^2 and 0.0267 cm^2.

4.4 Saturation of Lithium Hydroxide Solutions with Hydrogen Gas

The saturation process is performed by bubbling hydrogen gas presaturated with water vapor through the electrolyte solution, the temperature of the system being controlled to within $\pm$ 0.05°C with a proportional controller. For concentrated lithium hydroxide solutions and at high temperatures, considerably longer saturation periods were required. For such cases, a saturation period of 45 to 60 minutes was used as compared to 20 to 30 minutes for dilute solutions.

4.5 Measurement of Diffusion and Residual Currents

The diffusion and residual currents were measured using a Sargent model XV polarograph. A constant predetermined voltage (corresponding to the middle of the plateau in the voltage-current curve) was applied; and the current recorded automatically. Six replications were made for each experiment. Between each measurement the solution was resaturated with hydrogen. The residual current was measured after the dissolved hydrogen had been stripped off with nitrogen gas. The constancy of the product $i_t\sqrt{t}$ was checked for each experiment, only those results which satisfied this criterion were accepted for calculation of diffusion coefficient. It should be pointed out that the electrodes

(both the microelectrode and the counter electrode) had to be cleaned periodically with concentrated sulfuric acid and rinsed with distilled water.

4.6 Results

The results of these experiments are given in Table 4.1 and in Figure 4.1. The deviations given are standard deviation from the arithmetic mean of six replications. The values at 25°C represent the averages of twelve replications for each concentration using two microelectrodes. As expected the diffusion coefficients decrease with increase in lithium hydroxide concentration and increase with increase in temperature.

4.7 Discussion of Results

4.7.1 Modified Eyring Theory

Ratcliff and Holcroft[42] modified the Eyring reaction rate theory for diffusion for the special case of gas diffusion in electrolyte. The modified theory predicts that $\ell n\ D/D_o$ is a linear function of species fraction. Figures 4.2 through 4.4 show such plots for the present measurements. It can be seen that within experimental error, the experimental points lie approximately on a straight line.

4.7.2 Kinetic Theory of Diffusion

The kinetic theory discussed in the previous report[6] was used to predict the diffusion coefficients of hydrogen in lithium hydroxide solutions. It was found that the theory gives good predictions for concentration dependence. Owing to the nature of the hard sphere potential, it is expected that the theory cannot quantitatively predict temperature dependence of diffusion coefficients. Hence, the hard sphere

Table 4.1: Diffusion Coefficients of H_2 in LiOH Solutions

Wt. % LiOH	Normality of LiOH	Temperature			
		25°C	40°C	60°C	80°C
2.06	0.86	3.32 ± 0.049	4.95 ± 0.15	6.99 ± 0.097	--
4.10	1.81	2.95 ± 0.11	4.42 ± 0.083	6.32 ± 0.076	--
6.15	2.75	2.48 ± 0.08	3.78 ± 0.095	5.33 ± 0.072	--
7.7	3.5	2.195± 0.05	3.37 ± 0.03	4.72 ± 0.083	6.35 ± 0.05
10.05	4.62	1.85 ± 0.07	2.76 ± 0.02	4.02 ± 0.062	5.7 ± 0.15

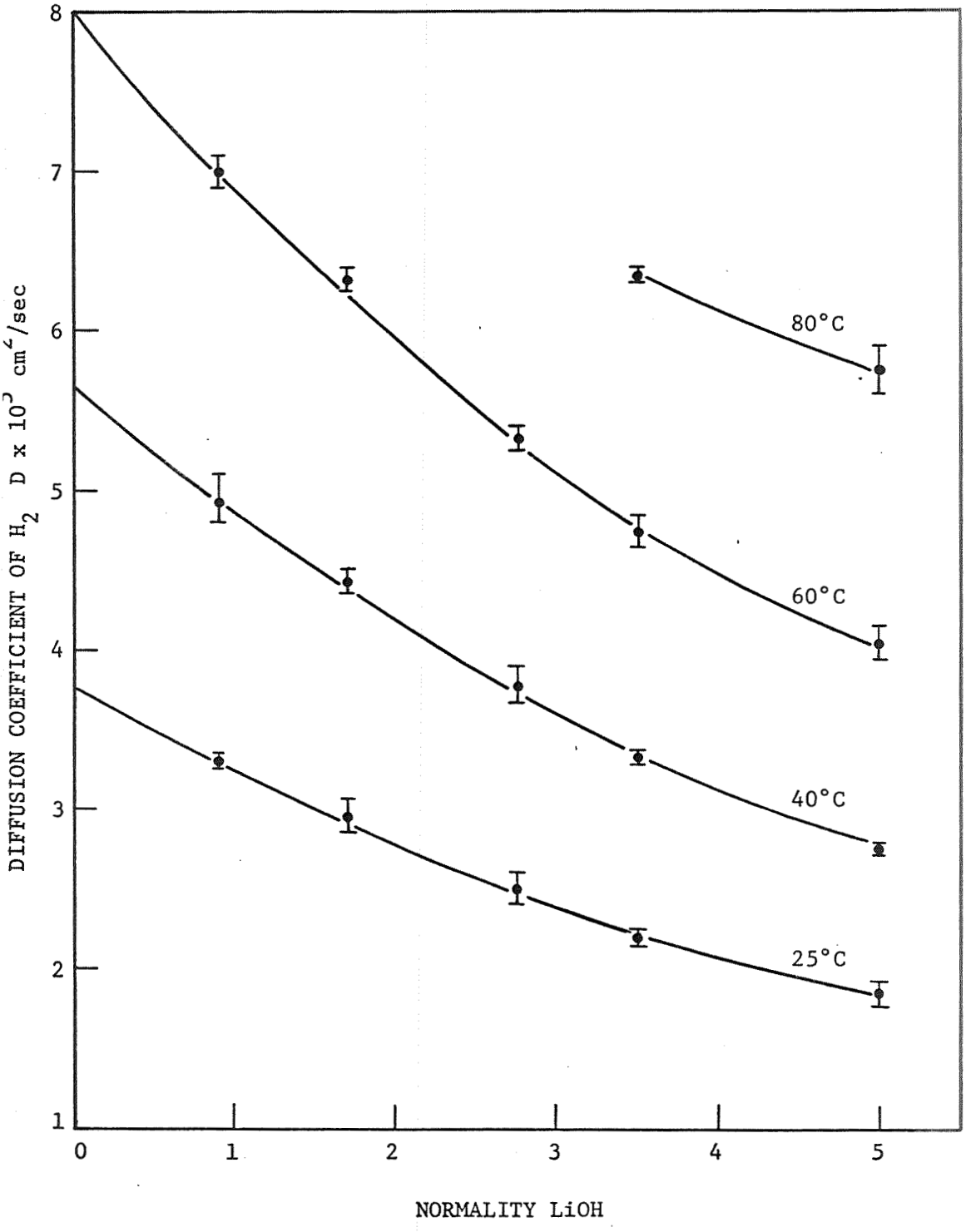

Figure 4.1. Diffusion Coefficients of Hydrogen in Lithium Hydroxide Solutions

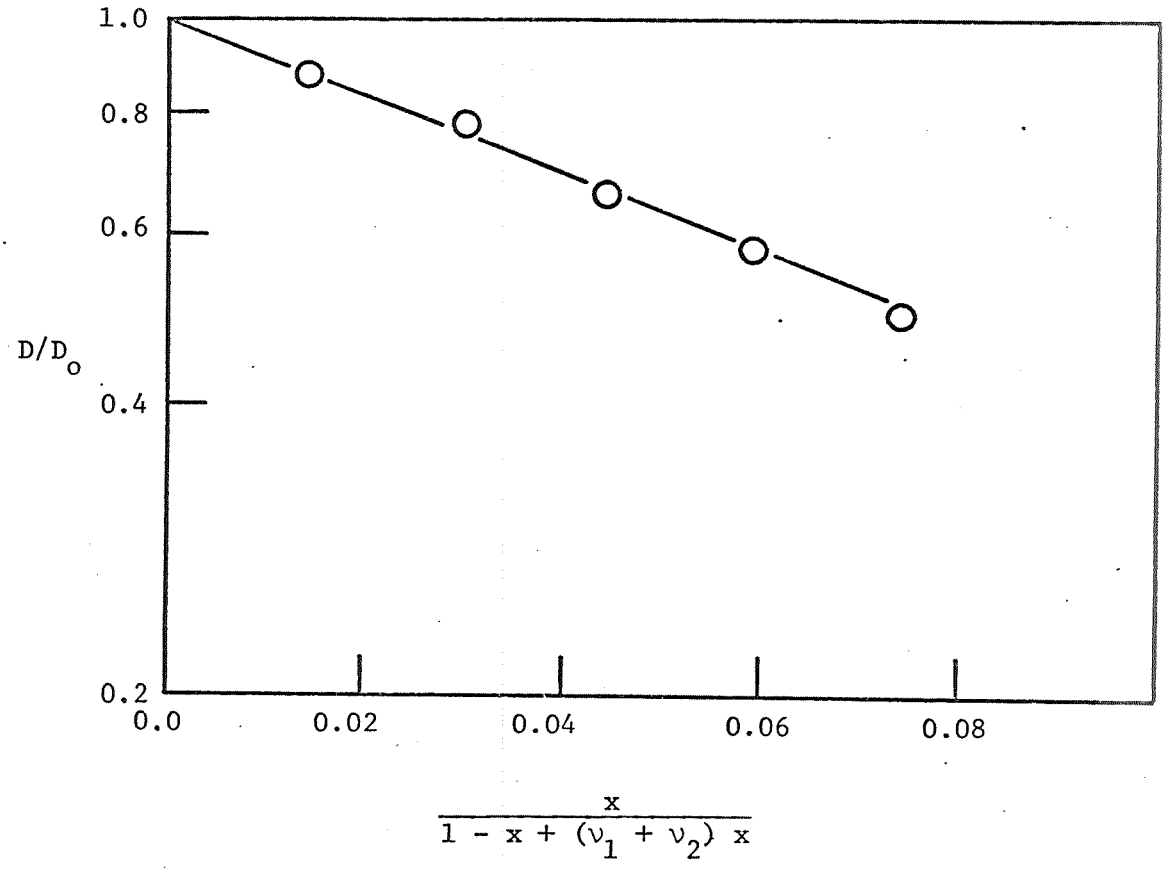

Figure 4.2. $\ell n\ D/D_o$ vs Species Fraction at 25°C.

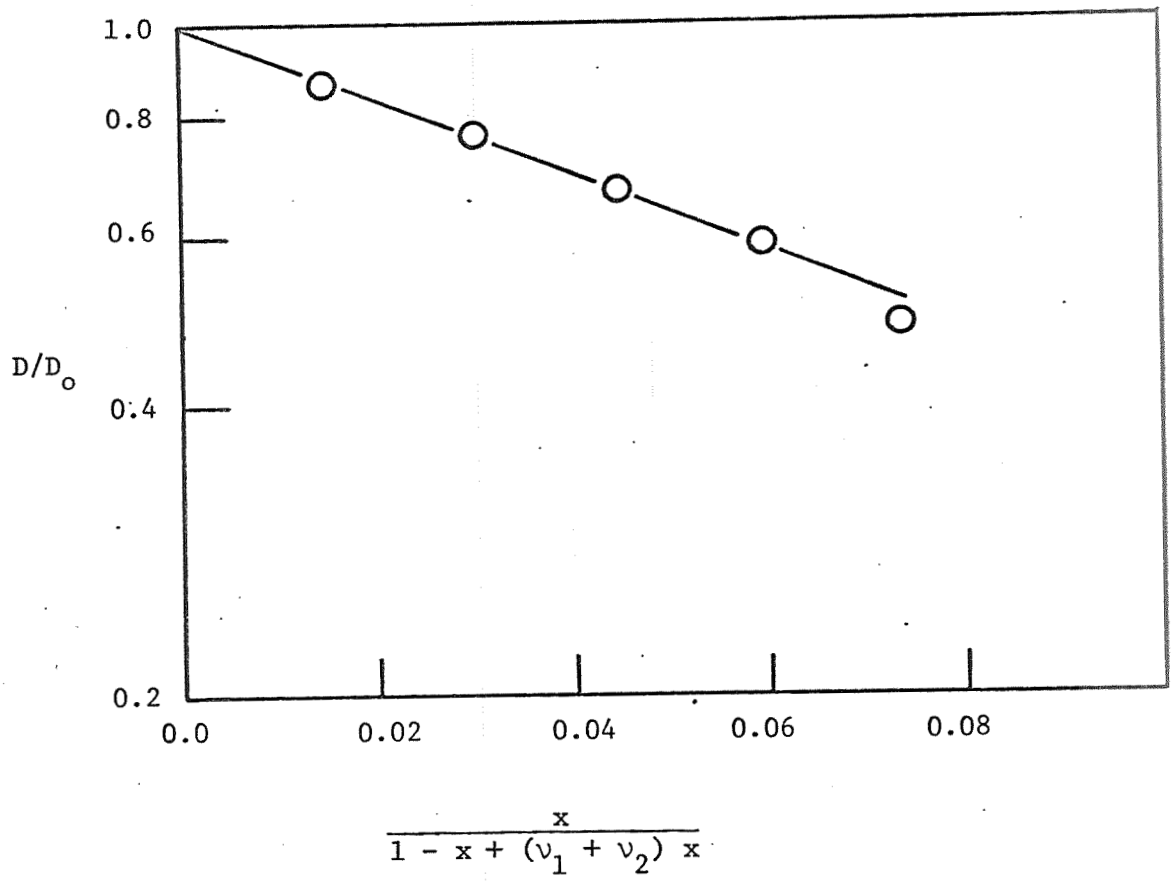

Figure 4.3. $\ell n\ D/D_o$ vs Species Fraction at 40°C.

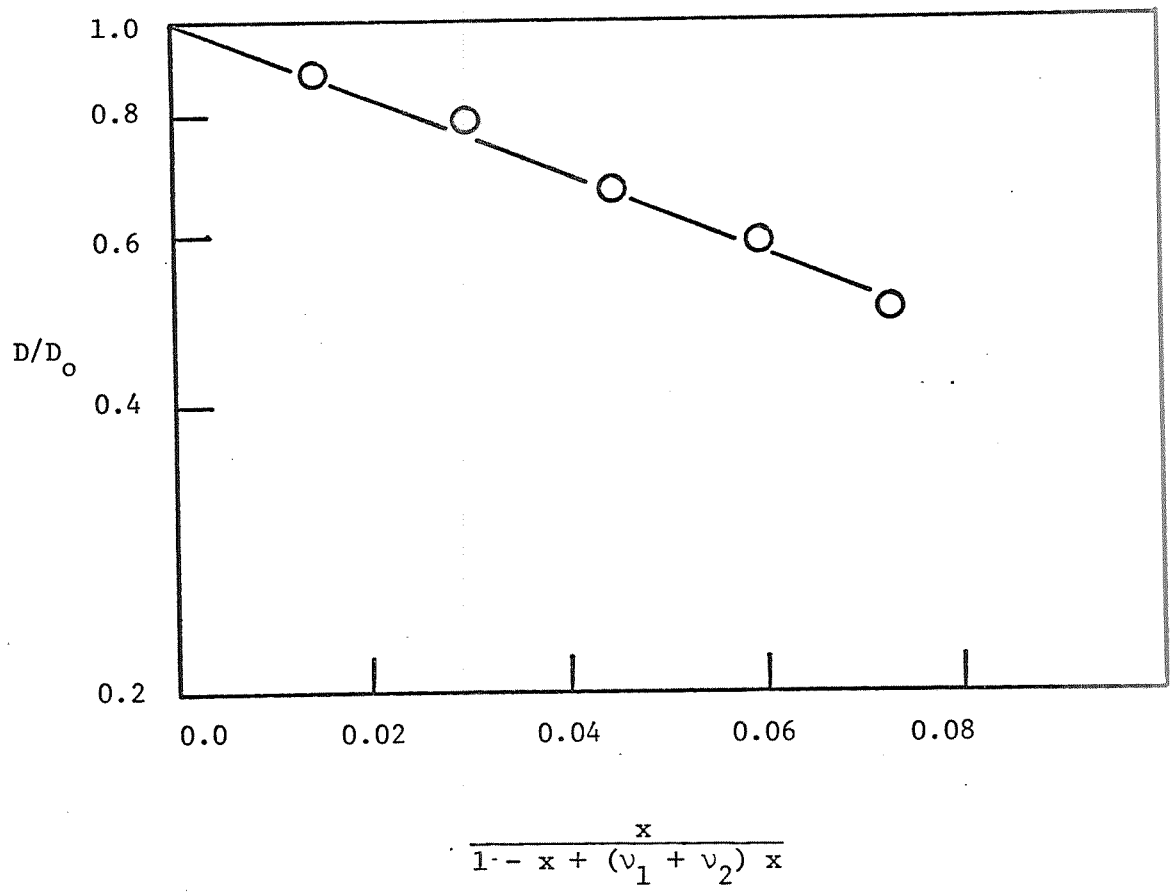

Figure 4.4. ℓn D/D_o vs Species Fraction at 60°C.

diameters were varied slightly (2 to 3%) in order to predict the proper diffusion coefficient of hydrogen in water. This is essentially a test of the theory for its ability to predict concentration dependence at various temperatures. It can be seen from Figure 4.5 that, as expected, the theory can predict proper concentration dependence.

The perturbation theory for equilibrium properties proposed by Barker and Henderson[43], which proved to be so successful in predicting equilibrium properties, gives an expression for a temperature dependent hard sphere diameter.

$$d = \int_0^{\sigma} (1 - e^{-\phi(r)/kT}) \, dr \qquad (4\text{-}1)$$

Even though using this temperature dependent hard sphere diameter improves the prediction considerably, it is still not sufficient to predict the sharp increase in diffusion coefficient with increase in temperature. This is to be expected for the equation above was arrived at from equilibrium consideration. Therefore, in order to predict the proper temperature dependence for the diffusion coefficient, a perturbation theory for transport properties has to be proposed, and this is being undertaken.

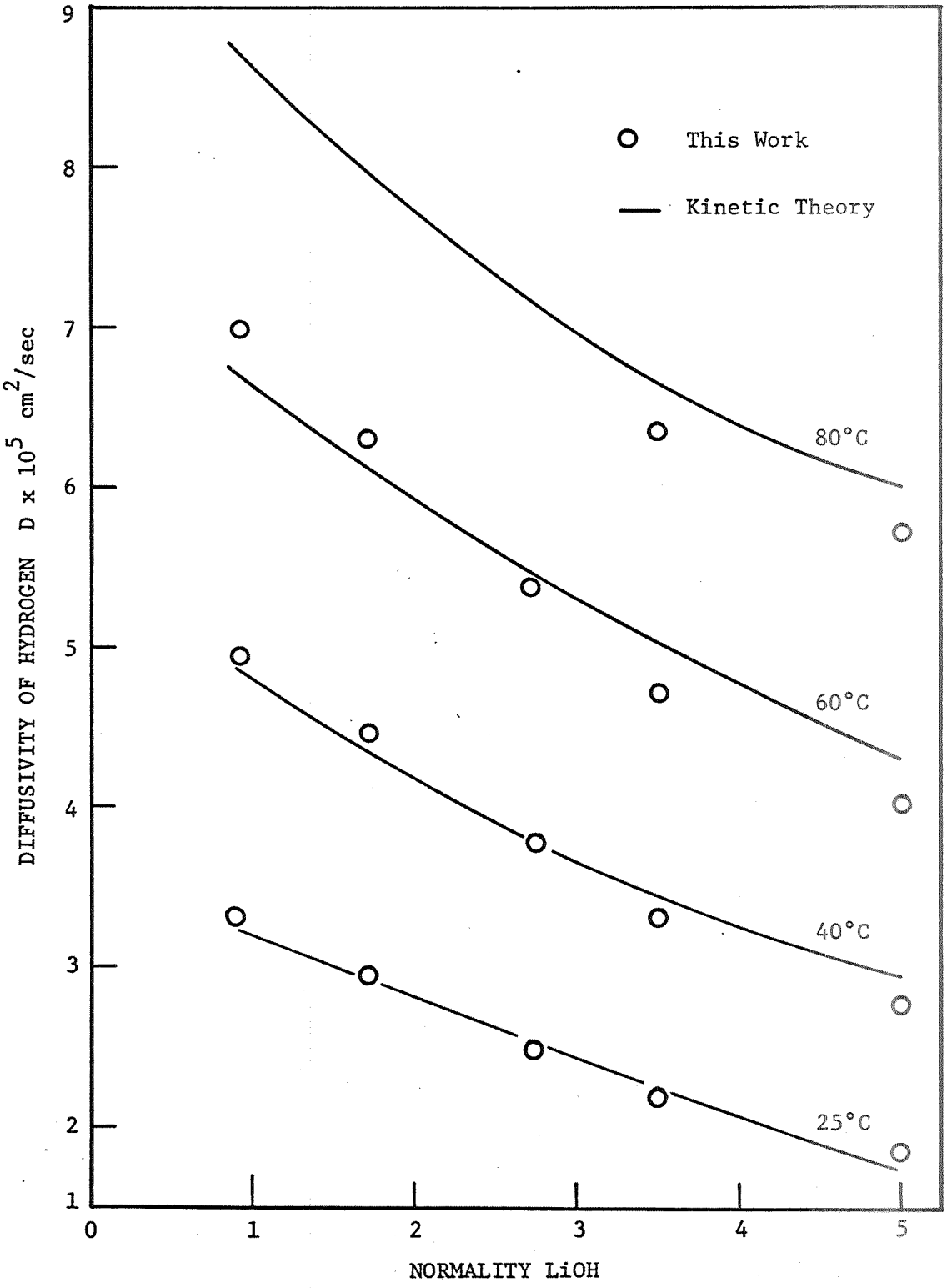

Figure 4.5. Prediction of Diffusion Coefficients Using Kinetic Theory

APPENDIX

I. Sample Calculation for Concentration Variable

5.61% KOH, 13.81% K_2CO_3, 80.58% H_2O

56.1 g KOH/1000 g solution

138.1 g K_2CO_3/1000 g solution

Molecular weight of KOH = 56.109

Molecular weight of K_2CO_3 = 138.213

$\therefore$ 1 mole of KOH $\rightleftharpoons$ 2 mole ions of KOH

$\therefore$ 1 mole of K_2CO_3 $\rightleftharpoons$ $\frac{3}{5}$ mole ions of K_2CO_3 / 5 total mole ions

Above solution has concentration of 5 mole ions/1000 grams

II. Sample Calculation for Analyses of Solutions

Both 5.0000 gram samples (titrated with 1.0 N HCl)

Total alkalinity titration 22 ml $\therefore$ 4.4 meg/gram solution

Total KOH titration 18 ml $\therefore$ 3.6 meg/gram solution

$\therefore$ 3.6 meg KOH/gram solution

and 4.4 - 3.6 = 0.8 meg K_2CO_3/gram solution

(3.6)(56.109)/10 = 20.2% KOH

(0.8)(138.213/2)/10 = 11.1% K_2CO_3

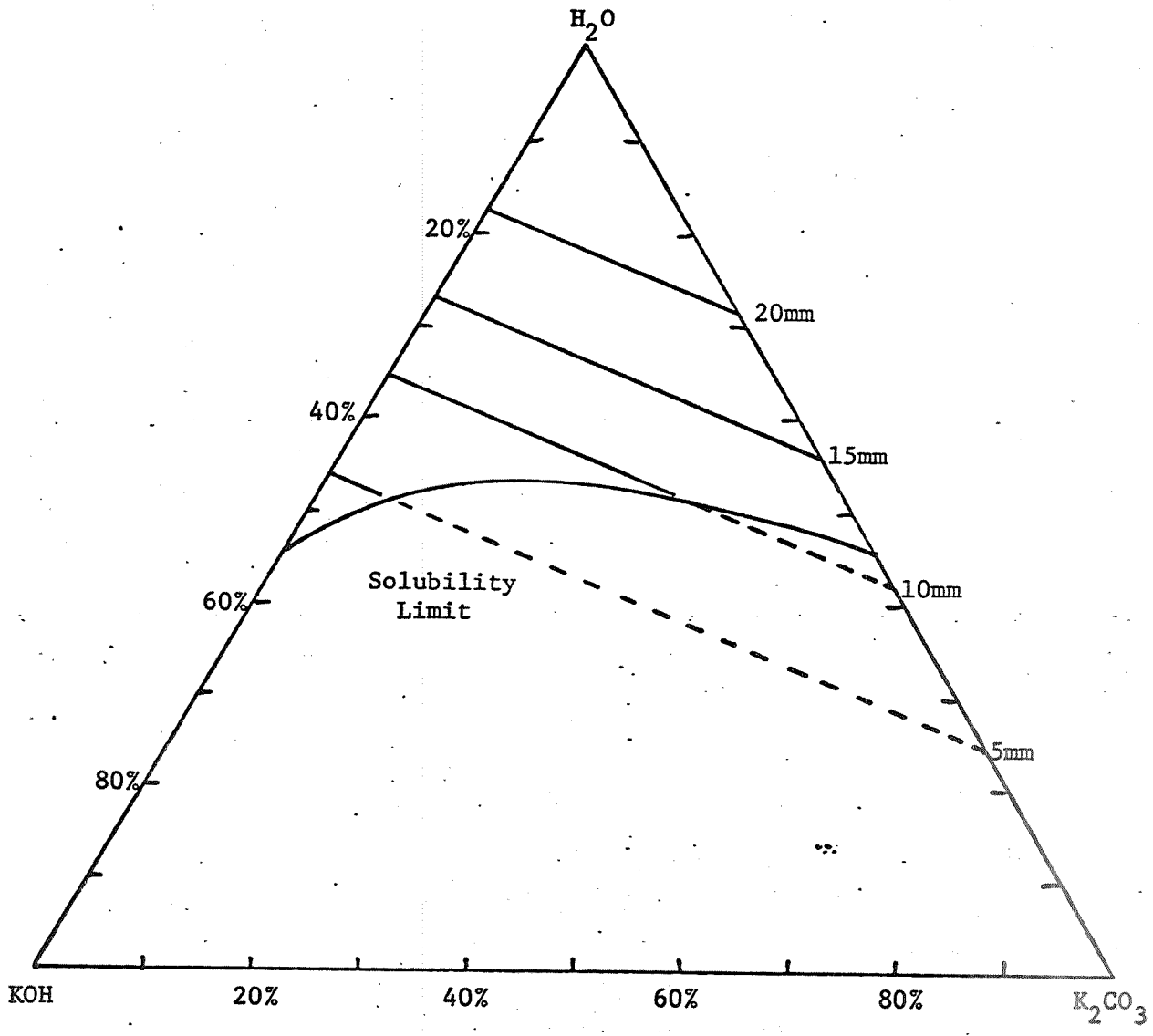

Figure A.1. Isobars on Triangular Plot at 25°C

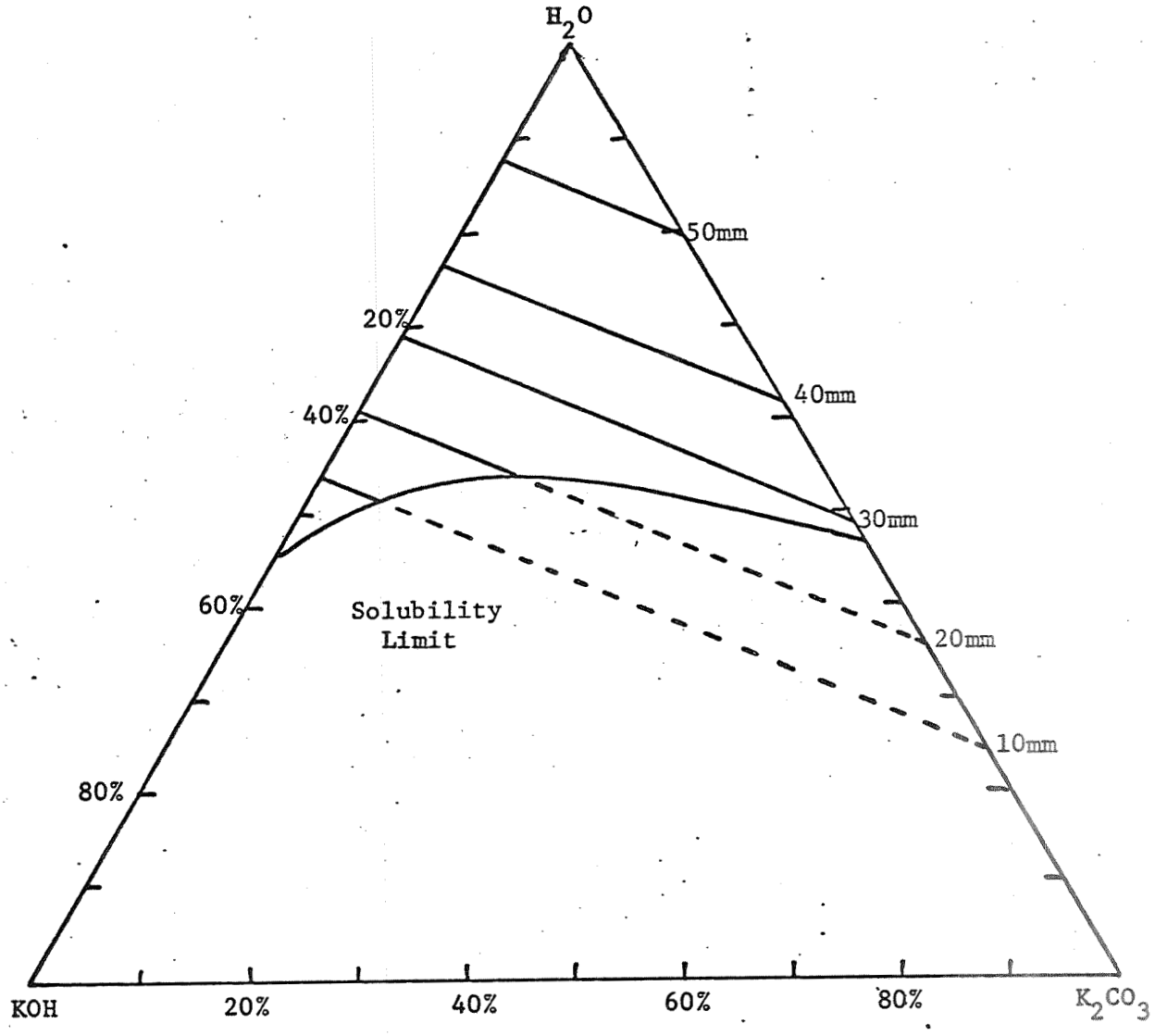

Figure A.2. Isobars on Triangular Plot at 40°C

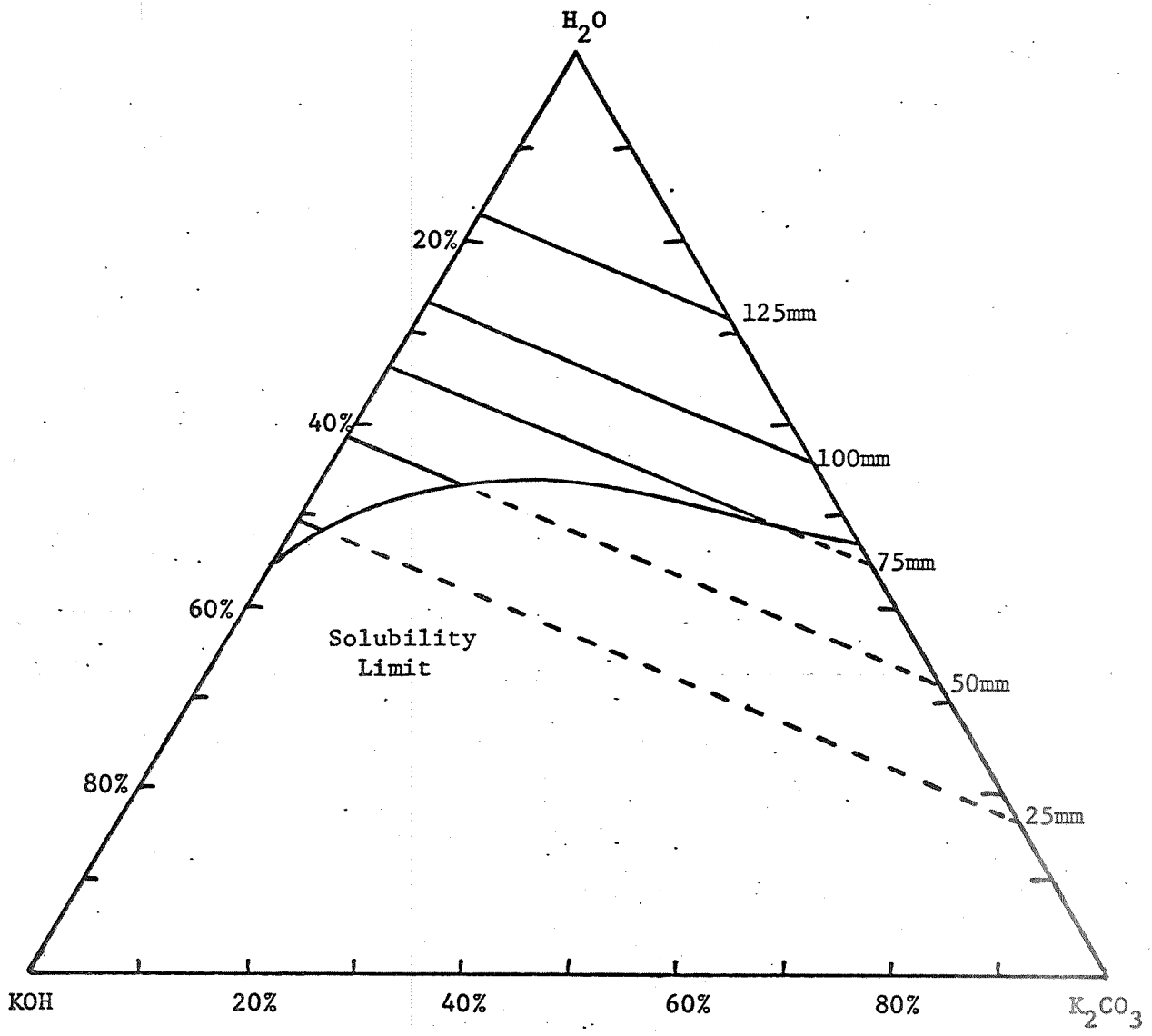

Figure A.3. Isobars on Triangular Plot at 60°C

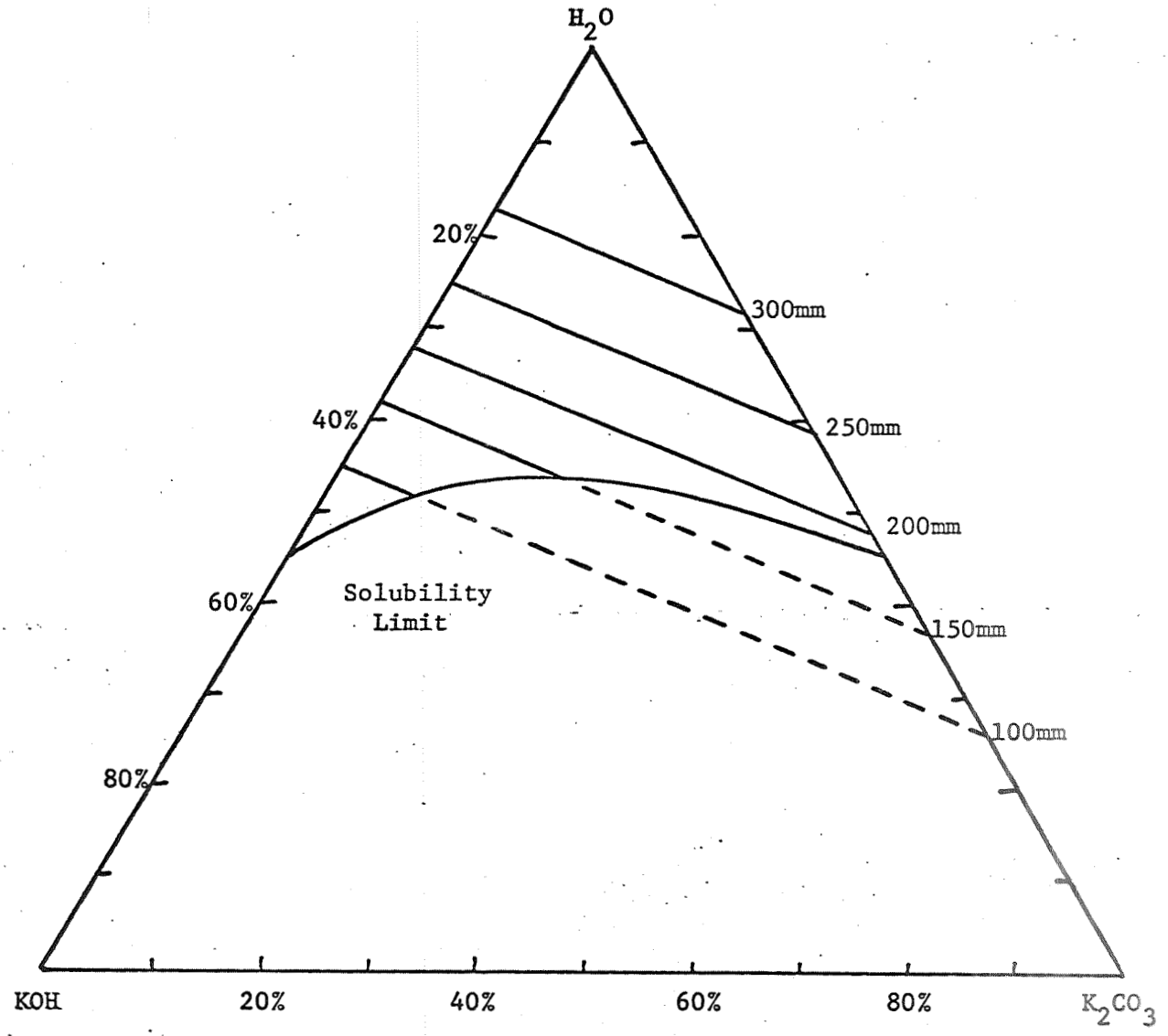

Figure A.4. Isobars on Triangular Plot at 80°C

```
      SUBROUTINE LESQ(Y,X)
      DOUBLE PRECISION A(11,11),B(11),C(11),P(20),TEMP,FACTOR,SUM
      COMMON C,IDEG(11),YS(200),DIFF(200),M,NUMBER,N,SS,GDV
      DIMENSION Y(200),X(200)
C
C     WHERE M IS THE DEGREE OF THE POLYNOMIAL
C     WHERE NUMBER IS THE NUMBER OF DATA POINTS
C     WHERE X AND Y ARE THE DATA PAIRS
C     WHERE A IS THE ARRAY FOR THE SUMS
C     WHERE B IS THE ARRAY FOR THE CONSTANT TERMS
C     WHERE C IS THE ARRAY FOR THE UNKNOWNS
C     WHERE P IS THE ARRAY FOR THE POWERS OF X
C     WHERE SS IS THE SUM OF SQUARES OF THE DEVIATIONS
C     WHERE GDV IS THE MAXIMUM DEVIATION
C
      DO 70 I=1,11
70    C(I)=0.0D 00
      MX2=M*2
      DO 13 I=1,MX2
      P(I)=0.0D 00
      DO 13 J=1,NUMBER
13    P(I)=P(I)+X(J)**I
      N=M+1
      DO 905 I=1,N
      IK=I
      IK=IK-1
905   IDEG(I)=IK
      DO 30 I=1,N
      DO 30 J=1,N
      K=I+J-2
      IF(K) 29,29,28
28    A(I,J)=P(K)
      GO TO 30
29    A(1,1)=NUMBER
30    CONTINUE
      B(1)=0.0D 00
      DO 21 J=1,NUMBER
21    B(1)=B(1)+Y(J)
      DO 22 I=2,N
      B(I)=0.0D 00
      DO 22 J=1,NUMBER
22    B(I)=B(I)+Y(J)*X(J)**(I-1)
      NMI=N-1
      DO 300 K=1,NMI
      KPI=K+1
      L=K
      DO 400 I=KPI,N
      IF(DABS(A(I,K))-DABS(A(L,K))) 400,400,401
401   L=I
400   CONTINUE
      IF(L-K) 500,500,405
```

```
405     DO 410 J=K,N
        TEMP=A(K,J)
        A(K,J)=A(L,J)
410     A(L,J)=TEMP
        TEMP=B(K)
        B(K)=B(L)
        B(L)=TEMP
500     DO 300 I=KPI,N
        FACTOR=A(I,K)/A(K,K)
        A(I,K)=0.0D 00
        DO 301 J=KPI,N
301     A(I,J)=A(I,J)-FACTOR*A(K,J)
300     B(I)=B(I)-FACTOR*B(K)
        C(N)=B(N)/A(N,N)
        I=NMI
710     IPI=I+1
        SUM=0.0D 00
        DO 700 J=IPI,N
700     SUM=SUM+A(I,J)*C(J)
        C(I)=(B(I)-SUM)/A(I,I)
        I=I-1
        IF(I) 800,800,710
800     CONTINUE
        SS=0.0
        GDV=0.0
        DO 100 IL=1,NUMBER
        YS(IL)=C(1)+C(2)*X(IL)+C(3)*X(IL)**2+C(4)*X(IL)**3+C(5)*X(I
                                                                  L)**4+
     1C(6)*X(IL)**5+C(7)*X(IL)**6+C(8)*X(IL)**7+C(9)*X(IL)**8+C(1
                                                                  0)*X(IL
     2)**9+C(11)*X(IL)**10
        DIFF(IL)=YS(IL)-Y(IL)
        IF(ABS(DIFF(IL)).GE.GDV) GDV=ABS(DIFF(IL))
100     SS=SS+DIFF(IL)**2
        RETURN
        END
```

References Cited

1. W. R. Bousfeld, Trans. Faraday Soc., 13, 401 (1918).
2. D. A. Sinclair, J. Phys. Chem., 37, 495 (1933).
3. A. C. Cumming, J. Chem. Soc., 95, 1772 (1909).
4. R. D. Walker, Jr., Fifth Semi-Annual Report, May, 1968, NASA Research Grant NGR 10-005-022.
5. Y. Kamino and M. Masaaki, Denki Kagakn, 36, 461 (1968).
6. R. D. Walker, Jr., Tenth Semi-Annual Report, October, 1970, NASA Research Grant NGL 10-005-022.
7. T. Enns, P. F. Scholander and E. D. Bradstreet, J. Phys. Chem., 69, 389 (1965).
8. W. J. Parkinson and N. De Nevers, Ind. Eng. Fund., 8, 709 (1969).
9. K. Angström, Wied. Ann., 15, 297 (1882).
10. K. Angström, Wied. Ann., 33, 223 (1888).
11. J. Horiuti, Sci. Papers Inst. Phys. Chem. Res. (Tokyo), 17, 125 (1931).
12. I. Kritchevsky and A. Ilinskaya, Acta Physicochim. USSR, 20, 327 (1945).
13. W. L. Masterton, J. Chem. Phys., 22, 1830 (1954).
14. R. Kobayashi and D. L. Katz, Ind. Eng. Chem., 45, 440 (1953).
15. J. E. Desnoyers, G. E. Pelletier and C. Jolicoeur, Can. J. Chem., 43, 3232 (1965).
16. W. Wen and J. H. Hung, J. Phys. Chem., 74, 170 (1970).

17. N. C. Deno and C. H. Spink, J. Chem. Phys., 67, 1347 (1963).

18. E. R. Nightingale, Jr., J. Phys. Chem., 66, 894 (1962).

19. E. Huckel and H. Scheaf, Z. Physik, Chem., 21, 326 (1959).

20. T. S. Sarno, R. K. Mohanty and J. C. Ahluwalia, Trans. Faraday Soc., 561, 2333 (1969).

21. T. Ackerman and F. Schreiner, Z. Electrochem., 62, 1143 (1958).

22. S. Lindenbaum and G. E. Boyd, J. Phys. Chem., 68, 911 (1964).

23. H. S. Frank, J. Phys. Chem., 67, 1554 (1963).

24. L. M. Blair and J. A. Quinn, Rev. Sci. Inst., 39, 75 (1968).

25. A. Ben-Naim, J. Phys. Chem., 71, 1137 (1967).

26. W. Drost-Hanson, Private Communication, April, 1971.

27. G. Nemethy and H. A. Scheraga, J. Chem. Phys., 36, 3401 (1962).

28. A. Wishima, J. Phys. Chem., 67, 2079 (1963).

29. J. E. Desnoyers and F. M. Ichhaporia, Can. J. Chem., 47, 4639 (1969).

30. J. E. Jolly and J. H. Hildebrand, J. Amer. Chem. Soc., 80, 1050 (1958).

31. J. Walkley and J. H. Hildebrand, J. Amer. Chem. Soc.,81, 4439 (1959).

32. J. C. Gjaldbaek and J. H. Hildebrand, J. Amer. Chem. Soc., 72, 1077 (1950).

33. H. Hiroaka and J. H. Hildebrand, J. Phys. Chem., 67, 1919 (1963).

34. J. Walkley and W. I. Jenkins, Trans. Faraday Soc., 64, 19 (1968).

35. W. Y. Ng and J. Walkley, J. Phys. Chem., 73, 2274 (1969).

36. R. G. Linford and J. H. Hildebrand, Trans. Faraday Soc., 65, 1470 (1969).

37. R. H. Schumm and O. L. I. Brown, J. Amer. Chem. Soc., 75, 2520 (1953).

38. J. F. Connolly and G. A. Kandalic, CEP Symposium Series, 59, #44, 8 (1963).

39. T. D. O'Sullivan and N. O. Smith, J. Phys. Chem., 74, 1460 (1970).

40. E. W. Lyckman, C. A. Eckert and J. M. Prausnitz, Chem. Eng. Sci., 20, 703 (1965).

41. R. D. Walker, Jr., Sixth Semi-Annual Report, February, 1969, NASA Research Grant NGR 10-005-022.

42. G. A. Ratcliff and J. G. Holcroft, Trans. Inst. Chem. Engrs. (London), 41, 315 (1963).

43. J. A. Barker and D. Henderson, J. Chem. Phys. 47, 4714 (1967).

44. J. H. Dymond and E. B. Smith, The Virial Coefficients of Gases, Clarendon Press, Oxford (1969).